

*Full Length Research Paper*

# **Design, realization and optimization of a photovoltaic system equipped with analog maximum power point tracking (MPPT) command and detection circuit of the dysfunction and convergence the system (CDCS)**

**T. Mrabti<sup>1</sup>, M. El Ouariachi<sup>1</sup>, R. Malek<sup>1</sup>, Ka. Kassmi<sup>1</sup>, B. Tidhaf<sup>1</sup>, F. Bagui<sup>2</sup>, F. Olivié<sup>3</sup> and K. Kassmi<sup>1\*</sup>**

<sup>1</sup>Université Mohamed Premier, Faculté des Sciences, dept de Physique, Laboratoire LETAS, Oujda, Maroc.

<sup>2</sup>Laboratoire IRISE, Ecole d'Ingénieurs Ei CESI, Rouen, France.

<sup>3</sup>Université de TOULOUSE, Laboratoire d'analyse et d'architecture des systèmes (LAAS) CNRS: UPR8001 – Université Paul Sabatier - Toulouse III – Institut National Polytechnique de Toulouse-INPT–Institut National des Sciences Appliquées de Toulouse, France.

Accepted 29 July, 2011

**In this paper, we analyze the design, realization and optimization of a photovoltaic (PV) system equipped with a maximum power point tracking (MPPT) command and detection circuit of dysfunction and convergence the system (CDCS) to the new maximum power point (MPP) following a perturbation due to the meteorological variation (solar radiation, temperature, ..) and the load. We have analyzed in depth manner the structure and optimization the operation of the MPPT command realized during this work. The results obtained show very good agreement between simulation and experiment. The experimental system realized during cloudy days or by varying the load, shows that it operates under optimum conditions independently of the meteorological variations. At each perturbation, the CDCS circuit detects it and convergences the system without restart it. The good efficiency of the direct current to direct current (DC-DC) converter used and the low loss (less than 7%) shows that the system realized can be used in a PV system to minimize losses due to connecting the panels to the load and in particularly to minimize the cost of installations.**

**Key words:** Panels and photovoltaic system, photovoltaic conversion, maximum power point tracking (MPPT) command, the detection circuit of dysfunction and convergence (CDCS), direct current to direct current (DC-DC) converter, simulator Pspice, optimal functioning, energy losses.

## **INTRODUCTION**

The exhaustion of traditional energy resources such as gas and oil, and the pollution caused by these forms of energy on the environment have led the scientists to bend over to other sources of inexhaustible energy, abundant and clean. Renewable energies represent a realistic alternative that allows answering exhaustion resources of traditional energies, and the impact on the environment (Uyigüe and Archibong, 2010). The photo-

voltaic (PV) energy is a solution among the promising energy options with advantages such as abundance, the absence of any pollution and the availability in large quantities in anywhere of the globe worldly. Currently in the PV systems, the major problem is the transfer of the maximum power from PV generator to the load. In most cases, these systems suffer from lack of optimization and bad adaptation. The operating point that emerges is sometimes very far from the maximum power point (MPP). Among the solutions that exist in the literature, is the realization of an adaptation block between the PV generator and the load (Salameh et al., 1991; Kuei-Hsiang

\*Corresponding author. E-mail: [khkassmi@yahoo.fr](mailto:khkassmi@yahoo.fr).

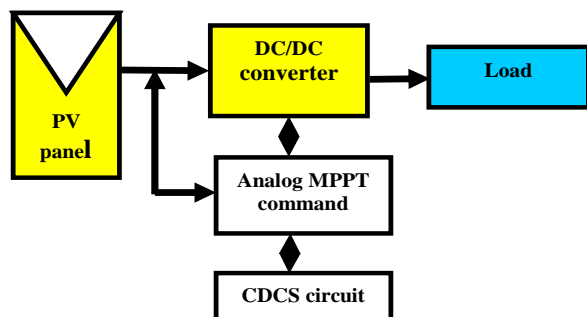


**Figure 1.** Synoptic diagram of the PV system equipped with a MPPT command and CDCS circuit.

and Ching-Ju, 2010; Damak et al., 2009; Neil et al., 2010; Shraif, 2002; Kalirasu and Dash, 2011). This block consists of a direct current to direct current (DC-DC) converter and an analogical maximum power point tracking (MPPT) command (Salameh et al., 1991; Shraif, 2002; El Ouariachi et al., 2009a; Mrabti et al., 2010; El Ouariachi et al., 2009b; Mrabti et al., 2009; El Ouariachi et al., 2010) or digital MPPT (Kuei-Hsiang and Ching-Ju, 2010; Dasgupta et al., 2008; Houssamo et al., 2010; Yaden et al., 2011; Gules et al., 2008; Dorin et al., 2011; Enrique et al., 2010; Ellouze et al., 2010). In both cases (analogical command or digital), the PV systems are not reliable and optimized, and diverge due to a sudden change of solar radiation and load. In the case of analogical MPPT commands, detection circuits of dysfunction are proposed in the literature (Shraif, 2002), but their disadvantage is that they restart the system when an eventual dysfunction occurs. Besides, the study of PV systems requires a prior detailed analysis fine of PV generators used. Currently, we have found in the literature very few results concerning the precise modeling of the electrical operation of PV panels as a function of meteorological conditions (solar radiation, temperature ...). Generally, there is a disagreement of an author to another (Shmilovitz, 2005; Huang et al., 2006), especially, concerning the influence of solar radiation on the optimal voltage of PV generators. Practically, most authors consider that the optimal voltage of PV generators is independent of the solar radiation. To better interpret the results of PV systems designed and realized in this work, we have studied the optimization of operation of the PV generator that were used in the system (Mrabti et al., 2010a; Mrabti, et al., 2010b; Kassmi et al., 2007a; Kassmi et al., 2007b). We have shown that the optimal voltage of PV panel depends heavily on weather conditions (solar radiation and temperature).

In this work, we studied the design and optimization of a PV system equipped with an analogical command and a circuit detection of dysfunction and convergence the system (CDCS) to the MPP of the PV panel without restarting the PV system. We have improved the structure,

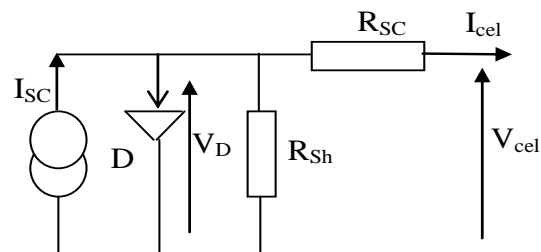


**Figure 2.** Electrical scheme of a PV cell.

structure, reliability and accuracy of the MPPT command used by Salameh et al., 1991 and Shraif, 2002). From the Pspice simulator and prototype realized in the laboratory, we have analyzed in a depth manner the optimal operation of the MPPT command and the possibility to detect a dysfunction at the time of the variation meteorological and the load, and instantaneous reconverge of the PV system to optimum conditions without restarting it. In order to valorize the results obtained, we estimated powers losses supplied by the PV panel from a full day of operation of the PV system realized in this work.

## PHOTOVOLTAIC SYSTEM

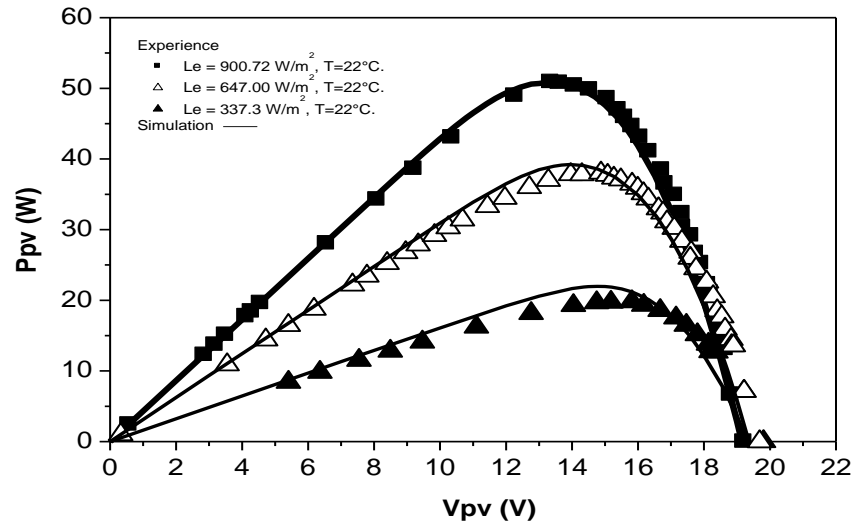
### Scheme synoptic of photovoltaic (PV) system

Figure 1 show a synoptic diagram of the PV system which is formed by:

- 1) PV panel (PV generator) characterized by MPP ( $V_{opt}$ ,  $I_{opt}$ ,  $P_{max}$  and  $R_{opt}$ ) for a given value of solar radiation and temperature (Mrabti et al., 2010b; Mrabti et al., 2010c; Kassmi et al., 2007a; Kassmi et al., 2007b)
- 2) The load which can either be two batteries (115Ah, 12V) in series, or a variable resistor ( $R_s$ ).
- 3) Power block that consists of a power boost DC-DC converter. Its operation in continuous mode is dimensioned at the frequency of 10 kHz (Mrabti et al., 2010a; El Ouariachi et al., 2009b; Mrabti et al., 2009; El Ouariachi et al., 2010; Narendran et al., 2010; Azmi and Aktacir, 2011).
- 4) An analogical MPPT command following the MPP of PV panel that depend on meteorological conditions and load variation. This MPPT command designed ensures proper regulation of the system around the MPP.
- 5) The CDCS of the PV system that allows to detect the dysfunction of the system (divergence of the system to close or open circuit conditions), following a sudden change of solar radiation or load, and to reconverge the PV system to its new MPP without restarting the system.

### Photovoltaic (PV) panel

In our study, we used and modeled the electrical properties of mono-crystalline PV panel (SP75) based on silicon materials (Mrabti et al., 2010a; Mrabti et al., 2010b, Kassmi et al., 2007a; Kassmi et al., 2007b). This panel is composed of 36 PV cells connected in series. The electrical model of a cell is shown in Figure 2. Each PV cell is formed by a DC generator ( $I_{sc}$  short-



**Figure 3.** Experimental (■, △, ▲) and simulated in Pspice (—) power-voltage characteristics. T, 22 to 25°C.

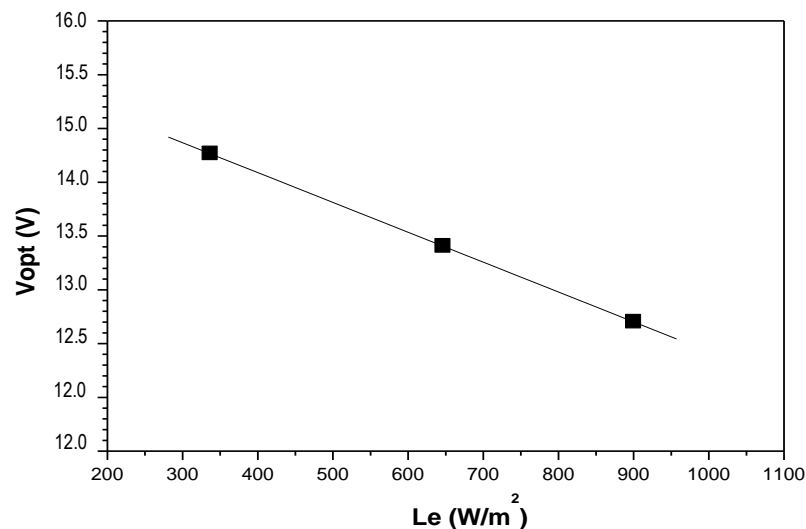


**Figure 4.** Variation of the optimal voltage ( $V_{opt}$ ) as a function of solar radiation. T, 22 to 25°C.

circuit current), a diode D, a shunt  $R_{sh}$  resistance characterizing the leakage current of the junction and a series  $R_{sc}$  resistor characterizing the contact losses. We have deduced the electrical parameters of a cell from the Pspice simulator, power-voltage experimental characteristics (Figure 3) and those ensured by the manufacturer. We have shown that the optimal  $V_{opt}$  voltage increases linearly with the solar radiation (Figure 4) (Shraif, 2002): when the solar radiation varies from 300 to 900  $W/m^2$ , the optimum voltage varies from 14.8 V to 13.2 V (a decrease of 11%).

#### Direct current to direct current (DC-DC) converter

The structure of DC-DC boost converter is shown in Figure 5. In this system:

- 1) The freewheeling diode (D) is a fast diode and supporting a current of 10 A. The various components of the converter (L, CE, CS) are dimensioned so that it operates at medium power (100 W) and a chopping frequency of 10 kHz.
- 2) The switch of the converter is a power MOSFET transistor. It is controlled by a signal of variable duty cycle [pulse width modulation (PWM)] and frequency of 10 kHz. We chose this transistor because it presents satisfactory performance: low power losses by switching and has a very low  $R_{Dson}$  resistance.

#### Structure and operation of the maximum power point tracking (MPPT) command

Figure 6 shows the synoptic diagram of the analogical MPPT

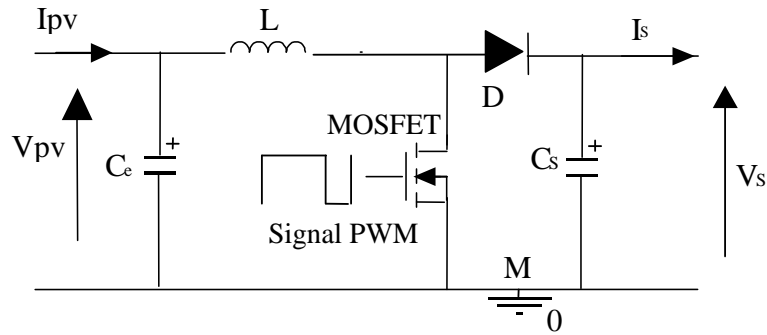


Figure 5. Boost DC-DC converter structure.

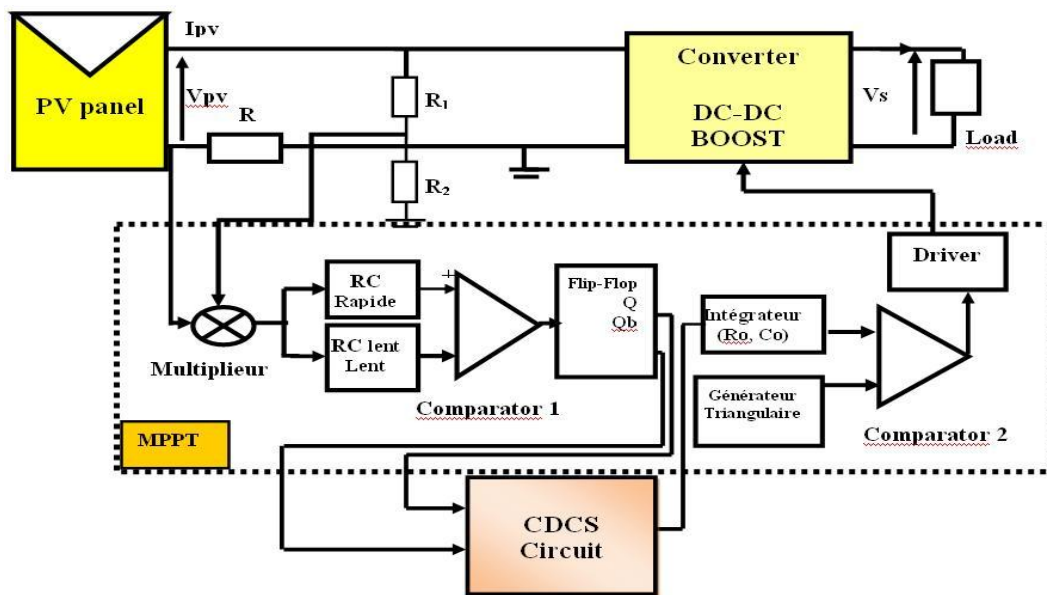


Figure 6. Block diagram of PV system equipped with an analogical MPPT command and CDCS.

command which is the subject of our study. According to El Ouariachi et al. (2009a), Mrabti et al. (2010a), El Ouariachi et al. (2009b), Mrabti et al. (2009) and El Ouariachi et al., 2010, we analyzed the feasibility of MPPT operation. In this work, we analyze its optimization: minimization of instabilities, noise.... This command consists of:

- 1) A shunt resistor ( $R$ ) of very low value that can withstand a current of 10 A. This shunt resistance allows having the  $I_{pv}$  current of PV panel since the voltage at its terminals is the image of the  $I_{pv}$  current.
- 2) A resistor bridge ( $R_1$  and  $R_2$ ) for taking a fraction of the voltage of PV generator.
- 3) A multiplier which provides at its output the image of the instantaneous power delivered by the PV generator.
- 4) Two integrators: one is fast with time  $\tau_R$  constant, and one slow with time  $\tau_L$  constant. The fast integration delivers at its output a homogeneous voltage to the power provided by PV panel, and the slow integrator provides at its output a delayed power  $P_I(t+dt)$ . The

comparison between these two powers ( $P_r$  and  $P_I$ ) allows deducing the direction of system evolution: an increase or decrease in the power of the PV panel. At a given instant  $t$ , if the  $P_r$  power is higher (lower) than  $P_I$  power then there is an increase (decrease) in power output of PV generator.

- 5) A comparator (1) whose role is to make the comparison between the  $P_r$  power and the delayed  $P_I$ , and provide a rectangular signal at its output.
- 6) A Flip-Flop whose Q output changes state on each rising edge of the clock signal which is the output of the comparator (1). When the system evolves towards a decrease in power, the Q output changes its state, in order to reverse the direction of system evolution.
- 7) Integrator ( $R_0, C_0$ ) with the capacitor charges and discharges slowly. It delivers at its output a voltage constituting the reference  $V_{ref}$  voltage.
- 8) A comparator (2) which generates a rectangular signal (PWM signal of variable duty cycle  $\alpha$ ), resulting from the comparison between the  $V_{ref}$  voltage and the saw tooth issued by an oscillator frequency of 10 kHz. The variation of  $\alpha$  duty cycle depends on the  $V_{ref}$  voltage: when  $V_{ref}$  voltage increases (decreases), the duty

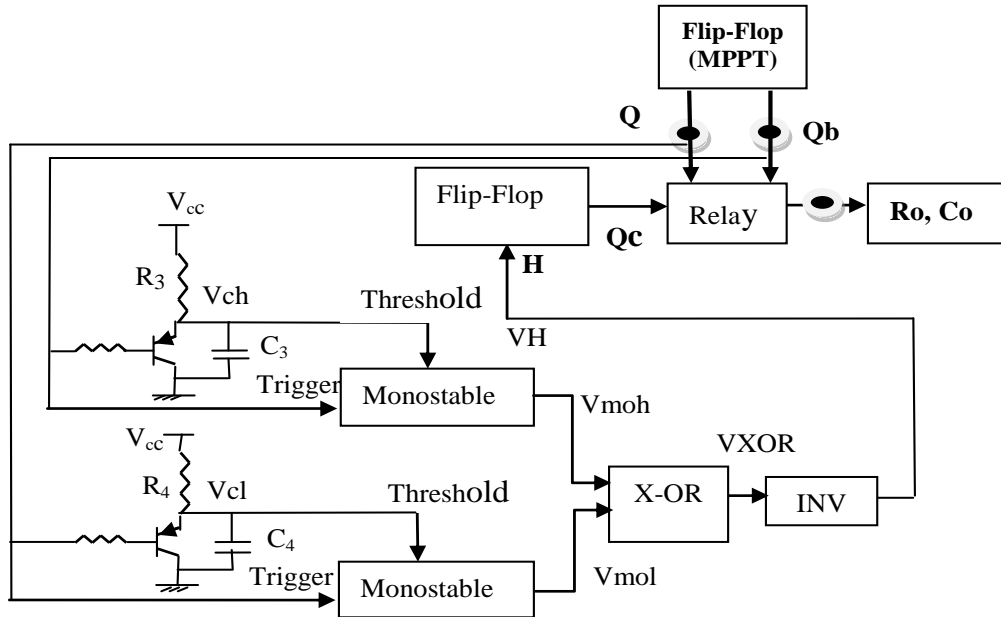


Figure 7. Schematic of CDCS.

cycle  $\alpha$  increases (decreases).

#### Structure and operation of the detection circuit of dysfunction and convergence the system. (CDCS)

In order to detect the dysfunction of PV system, we have improved the circuit used in the literature (Shraif, 2002) so that it ensures optimum operation without restarting the system. As shown in Figure 7, this circuit is formed by:

1) Two monostable detect the divergence of the PV system. The inputs of these monostables are connected to Q and Qb outputs of the Flip-Flop of the MPPT command. If the system diverges, the both outputs Q and Qb do not change state. The output of one monostable detects the divergence if the system diverges to the closed circuit conditions and the output of the other monostable detects if the system diverges to open circuit conditions. The duration of the detection of divergence is determined by the period of the monostable ( $T_1$  and  $T_2$ ) (<http://datasheet.-NE555.pdf>):

$$T_1 = 1.1 * R_1 * C_3 \quad T_2 = 1.1 * R_2 * C_4 \quad (1)$$

2) The outputs of the two monostable are connected to logic gate X-OR-type. If the system loses its optimum operating point, moments after  $T_1$  or  $T_2$ ) one of the two monostable changes state and accordingly, the output of X-OR gate changes. This shows that one of the monostables has detected the dysfunction of the PV system.

3) The output of gate X-OR is then inverted by a logic inverter. This pulse is applied to clock of 'Flip-Flop' and accordingly, the change of state at occur its Qc output.

4) The switching of the signal at the inverter output, changes the position of the blade of a relay which connects the input of the RoCo integrator to both Q outputs and Qb of the Flip-Flop of MPPT command. If the RoCo integrator is connected to the Q (Qb) output,

then the detection of a dysfunction reconnects the RoCo integrator at the output Qb (Q) of Flip-Flop of the MPPT command. This change in blade position of the relay induces change of direction of duty cycle variation of PWM signal generated by the MPPT command and thus, changes the direction of movement of the operating point of PV generator. This last movement allows the PV system converged to the new PPM following the sudden change in solar radiation or the load.

#### SIMULATION RESULTS OF THE PHOTOVOLTAIC (PV) SYSTEM IN PSPICE

##### Normal operation of the photovoltaic (PV) system without circuit of dysfunction and convergence the system (CDCS)

We implemented and simulated the electrical operation of the PV system of Figure 6 without the CDCS circuit, in the Pspice simulator for solar radiation of  $1000 \text{ W/m}^2$ , temperature of  $25^\circ\text{C}$  and a resistive load of  $50 \Omega$ . We noted the various electrical quantities and signals of the MPPT command when the RoCo integrator is connected either to the Q output or Qb output of the Flip-Flop. In both cases of connection (Q or Qb), we observed the same behavior of the PV system. Typical results of simulations are shown in Figures 8 and 9. It appears that:

1) The fast and slow integrators provide a homogeneous voltage to the instantaneous power (Pr) and delayed (PI). At each intersection of the two powers Pr and PI, the comparator (1) changes the state: if the Pr power is higher (lower) than PI, the output of comparator (1) switches to the down state (up) and the Q output of the Flip-Flop do not change (change) state. Also, if the Q output is in the high state (lower) the PV system evolution towards an increase (decrease) in the power of the PV panel.

2) The output voltage (Vref) of the RoCo integrator varies slowly. The comparison between this voltage and that provided by an oscillator ( $V_{osc}$ ), through the comparator (2) generates a rectangular signal PWM, width modulated, frequency of 10 kHz and

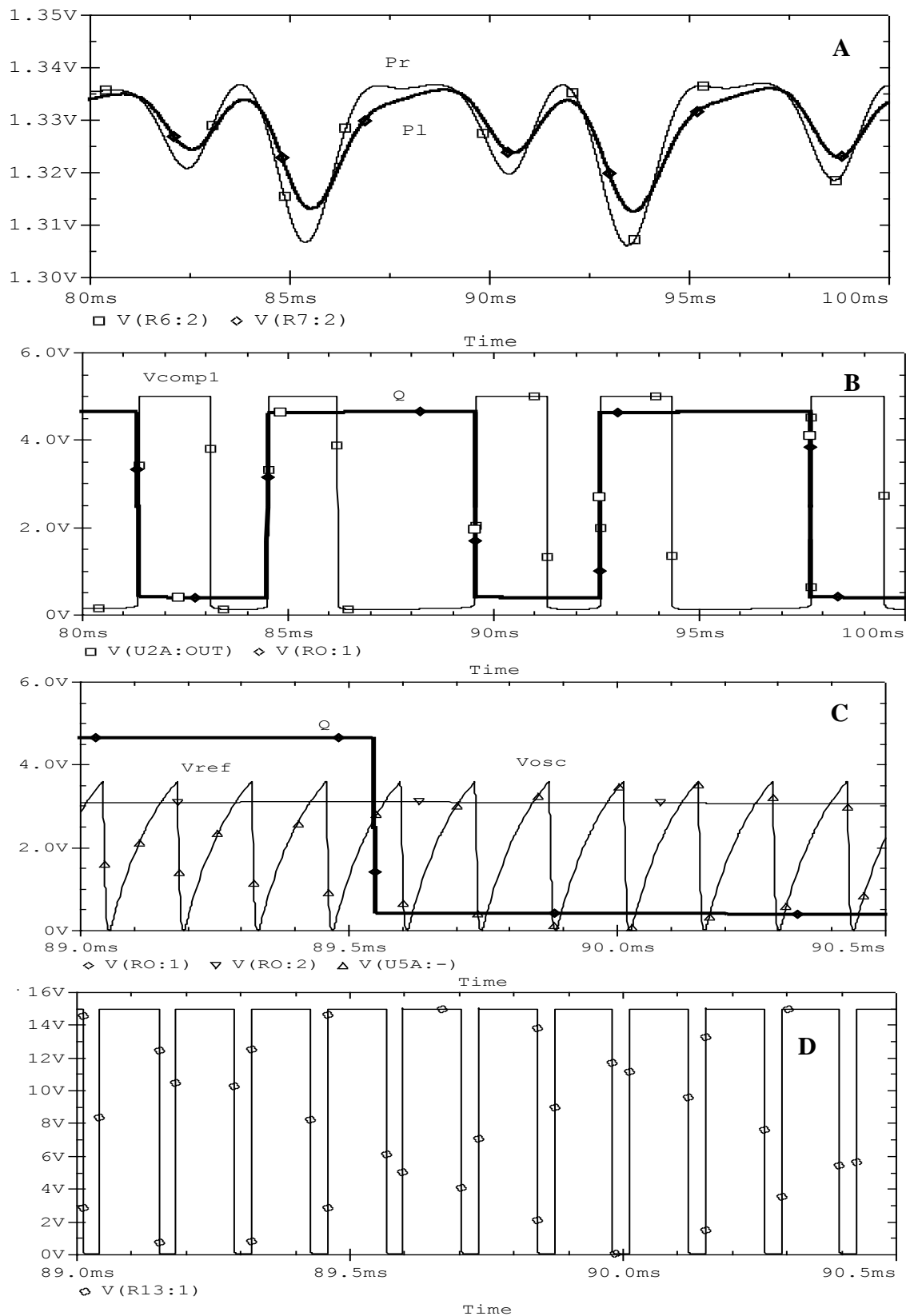


**Figure 8.** Typical signals obtained from Pspice simulator. A, Input of the comparator (1); B, output of the comparator 1(H) and the Flip-Flop (Q); C, input of the comparator 2 ( $Vref$ ,  $Vosc$ ) and the Output of the Flip-Flop (Q); D, PWM signal generated by the MPPT command.

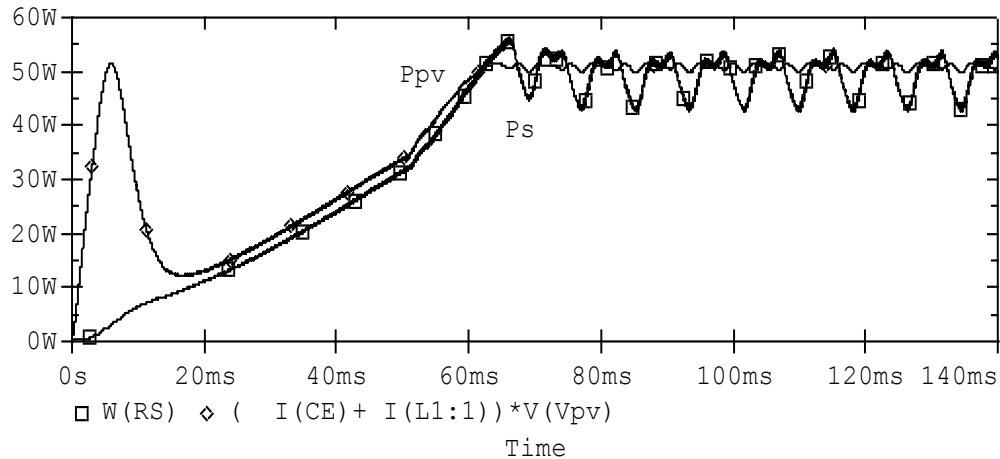


**Figure 9.** Typical simulation in Pspice of the powers to the input and output of the boost converter when the RoCo integrator is connected to the Q output of the Flip-Flop. Solar radiation,  $1000\text{W}/\text{m}^2$ ; T,  $25^\circ\text{C}$ ;  $R_s$ ,  $50\ \Omega$ .

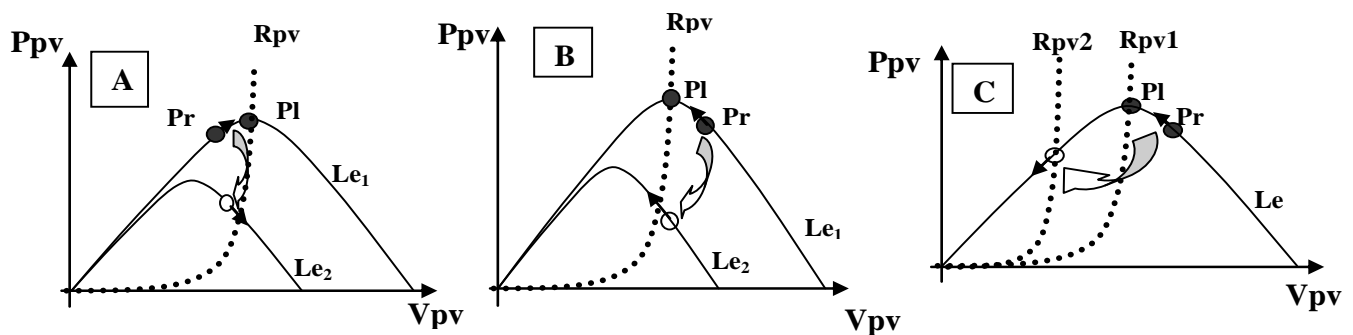


**Figure 10.** Situations of divergence of PV panels. A and B, following the variation of the solar radiation ( $Le_1 > Le_2$ ) for a load to the output panel ( $R_{pv}$ ); C, following the change of the load ( $R_{pv1} > R_{pv2}$ ) for the  $Le$  solar radiation; (—), power-voltage characteristic of PV panel; (- - -), power-voltage characteristic of a resistive load ( $R_{pv}$ ,  $R_{pv1}$ ,  $R_{pv2}$ ); Pr et Pl, instantaneous power and delayed.

the amplitude of 5 V. If the Q output is at down state (Up), the Vref voltage decreases (increases) and therefore, the duty cycle decreases (increases).

3) The simulation of electrical quantities (power) at the input and Output of the Boost converter shows that the system converges to the optimal conditions after a time of 60 ms. We have checked that the amplitude of oscillations depends on the values of the fast time constants ( $\tau_R$ ), slow ( $\tau_L$ ) and time constant ( $\tau_o$ ) of the RoCo integrator: when  $\tau_R$  and  $\tau_L$  are close (remote) and  $\tau_o$  important (small) the oscillations decreases (increases).

### Divergence of the photovoltaic (PV) system

In an abrupt change of solar radiation or the load, the PV system of Figure 6 can be diverge to the closed circuit conditions ( $\alpha = 1$ ) or open circuit ( $\alpha = 0$ ). Figure 10 shows the situations of divergence of the PV panel, observed on the simulator Pspice, following to changes in solar radiation (Figure 10A and B) or load (Figure 10C). When the variation of the solar radiation and the system evolves towards the open circuit conditions (Closed), and if the

instantaneous Pr power is less than PI delayed, then the PV panel diverges. Therefore, the system operates without the comparator (1) (Figure 6) compares the Pr power and PI ( $Pr$  lower than PI) and the Q output of Flip-Flop changes at the down state (Up). Similarly, when the variation of the load and the PV panel diverge toward the closed circuit conditions, the Q output of Flip-Flop get blocked in the Up state. Both situations induce the power losses supplied by the panels and stopping the PV system.

We studied the divergence of PV systems from the Pspice simulator system by imposing an abrupt change of solar radiation on one hand and the load on the other hand. The typical results obtained are shown in Figure 11 for solar radiation change. It appears when the variation of the solar radiation, the Q output of Flip-Flop blocked at the down state and the system diverges to open circuit conditions ( $\alpha = 0$ ). From the simulation of powers PI and Pr, and the Q output of Flip-Flop around the change of the solar radiation at time  $t = 120\ \text{ms}$  (Figure 12), we can conclude that the evolution of the system is one in Figure 10A: the variation of solar radiation occurred when the system was evolving towards open circuit conditions.

Simulation results show that the PV system equipped with an analog MPPT command diverges following to sudden changes in

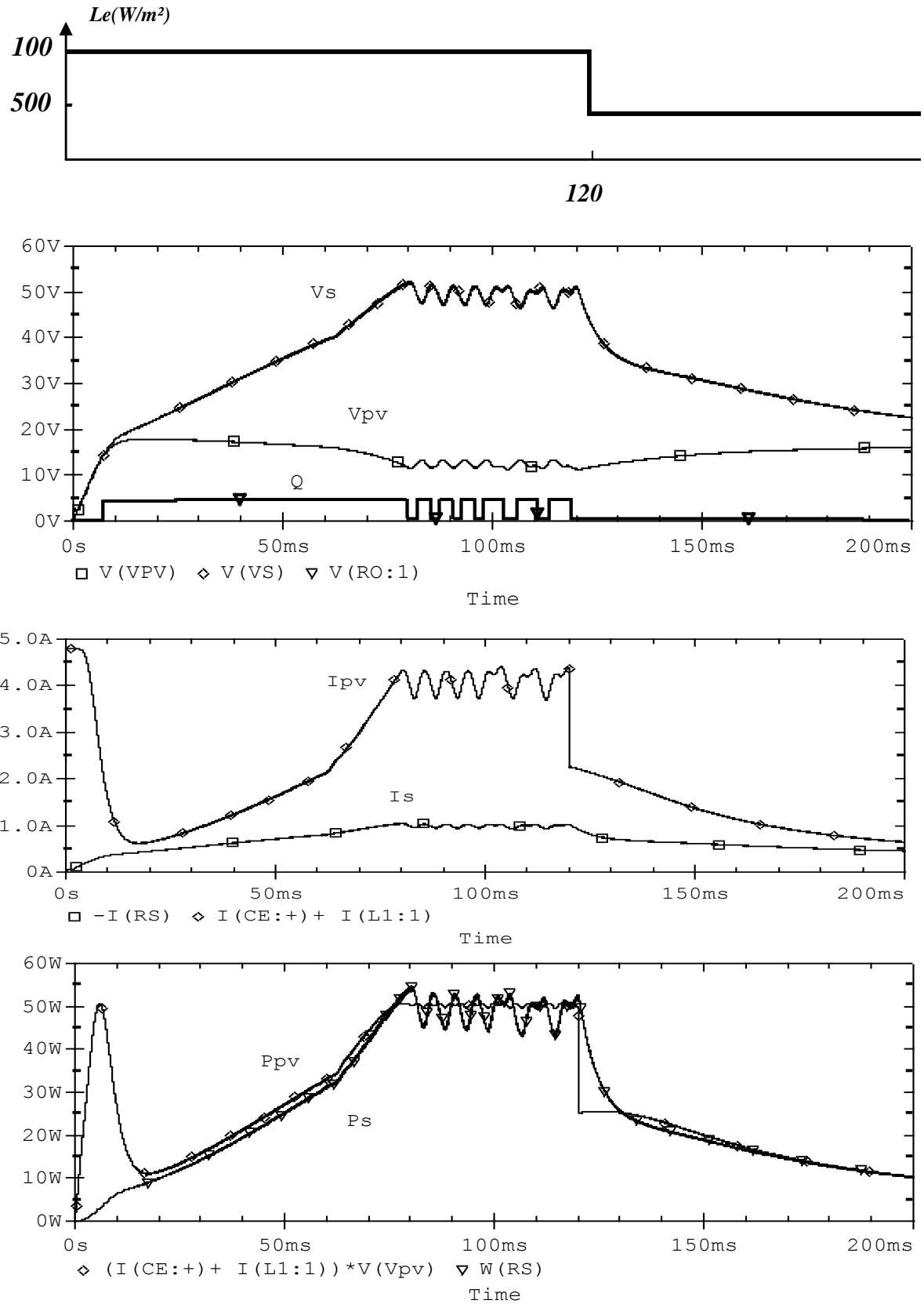


**Figure 11.** Pspice simulation of electrical quantities (voltage, current, power) at the input and output of the Boost converter, during the variation of the solar radiation ( $Le$ ) from 1000 W/m<sup>2</sup> to 500 W/m<sup>2</sup>. T, 25°C;  $R_s$ , 50  $\Omega$ .

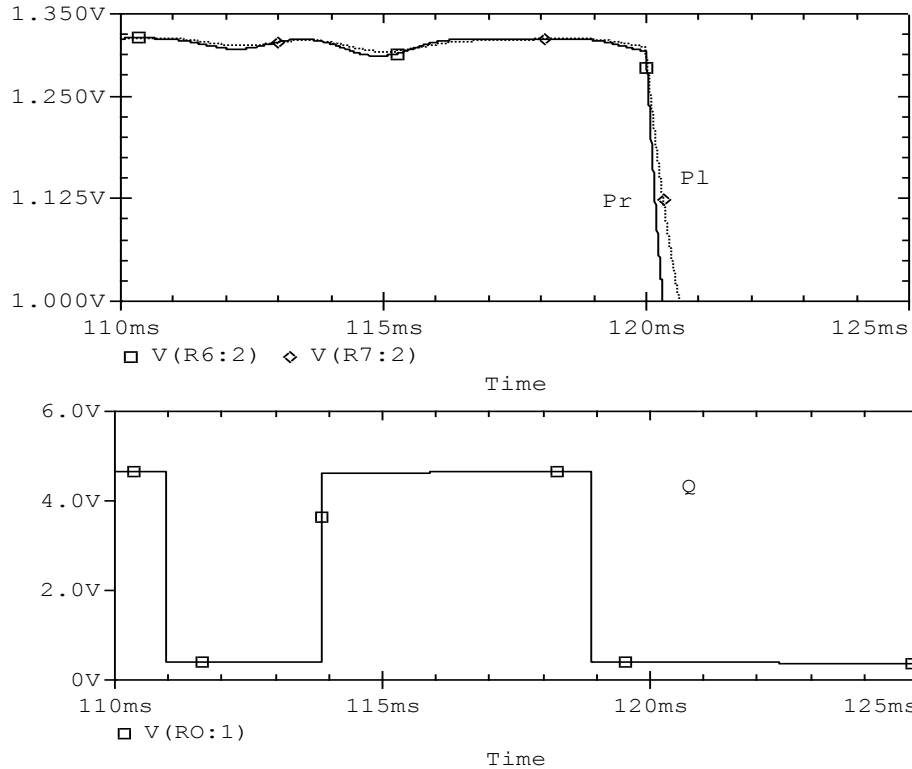


**Figure 12.** Powers Pr and PI, and the Q output simulated in Pspice upon variation of the solar radiation.

solar radiation or load. This situation can manifest on PV installation. Therefore, the design and the realization of circuits for detecting divergence and instantaneous convergences towards the optimum conditions are essential.

### Photovoltaic (PV) system equipped with the detection circuit of dysfunction and convergence of the system (CDCS)

Here, we analyze the Pspice simulator of the operation of PV systems equipped with MPPT command (Figure 6) and the CDCS (Figure 7). We study the operation of various blocks of the PV system when it undergoes abrupt changes in solar radiation or load. The typical results obtained are shown in Figure 13 for change of solar radiation. It appears:

1) After a time of about 90 ms the electrical quantities of the PV system oscillate around the optimal quantities. This operation manifests until the time of the order of 120 ms, which corresponds to variations of the solar radiation (Figures 13 and 14). During this mode of operation, the pulses appear at the Q and Qb outputs of Flip-Flop of the MPPT command (Figure 14). These pulses trigger the monostable (Up and Down) of the CDCS circuit (Figure 7) and prevent the  $C_3$  and  $C_4$  capacitors (Figure 7) to load and the threshold voltage reach the tipping point (Figure 14). Therefore, the outputs of the monostable flip at the unstable state (Up), the output of XOR in the down state and the output of the inverter in the Up state. Since we used a Flip-Flop in CDCS circuit which function on the rising edge of the clock signal, the output of this Flip-Flop does not change state (Down state). Consequently, the relay is not activated and the RoCo integrator of the MPPT command remains

connected to the Q output of the Flip-Flop of the MPPT command (Initial state).

2) When the variation of the solar radiation (at  $t = 120$  ms), the PV system diverges and the Q output of Flip-Flop blocked the down state (Figure 13). Consequently, the high bipolar transistor of the CDCS circuit blocked and the  $C_3$  capacitor is charging. When the voltage at terminals of this capacitor reaches after a time of about 20 ms, fixed by  $C_3$  and  $R_3$  (Equation 1), the tipping threshold then the output of high monostable switches to stable state (Down). This time 20 ms, that we have fixed, corresponds well to the time of the divergence of the system and the switching of the high monostable demonstrates the detection of the divergence. Contrariwise, the down bipolar transistor conducted and the voltage at terminals of the  $C_4$  capacitor is that of the saturation voltage of the transistor (0.8 V). The down monostable remains at the unstable state (Up).

3) When the detection of the divergence, the output of XOR switches to the up state and that of the inverter (clock of the Flip-Flop) in the down state. This last pulse activates the Flip-Flop of the CDCS circuit and its Q output switches to the Up state. Consequently, the relay is activated and the RoCo integrator of the MPPT command is connected to a new Q output of the Flip-Flop of the MPPT command. During the phase of the divergence, the RoCo integrator was connected to the Q output of Flip-Flop of the MPPT command. Since it is in the down state, the system diverges to open circuit conditions (the panel voltage increases). Hence, the detection of the dysfunction and the RoCo integrator is connected to the Qb output which is at up state (Flip-Flop of the MPPT command), then the operating point of the panel change direction by moving to the closed circuit conditions. So, the panel voltages decreases and reconverge to optimal quantities. As with the preceding paragraph, as soon as the power Pr and PI intersect,

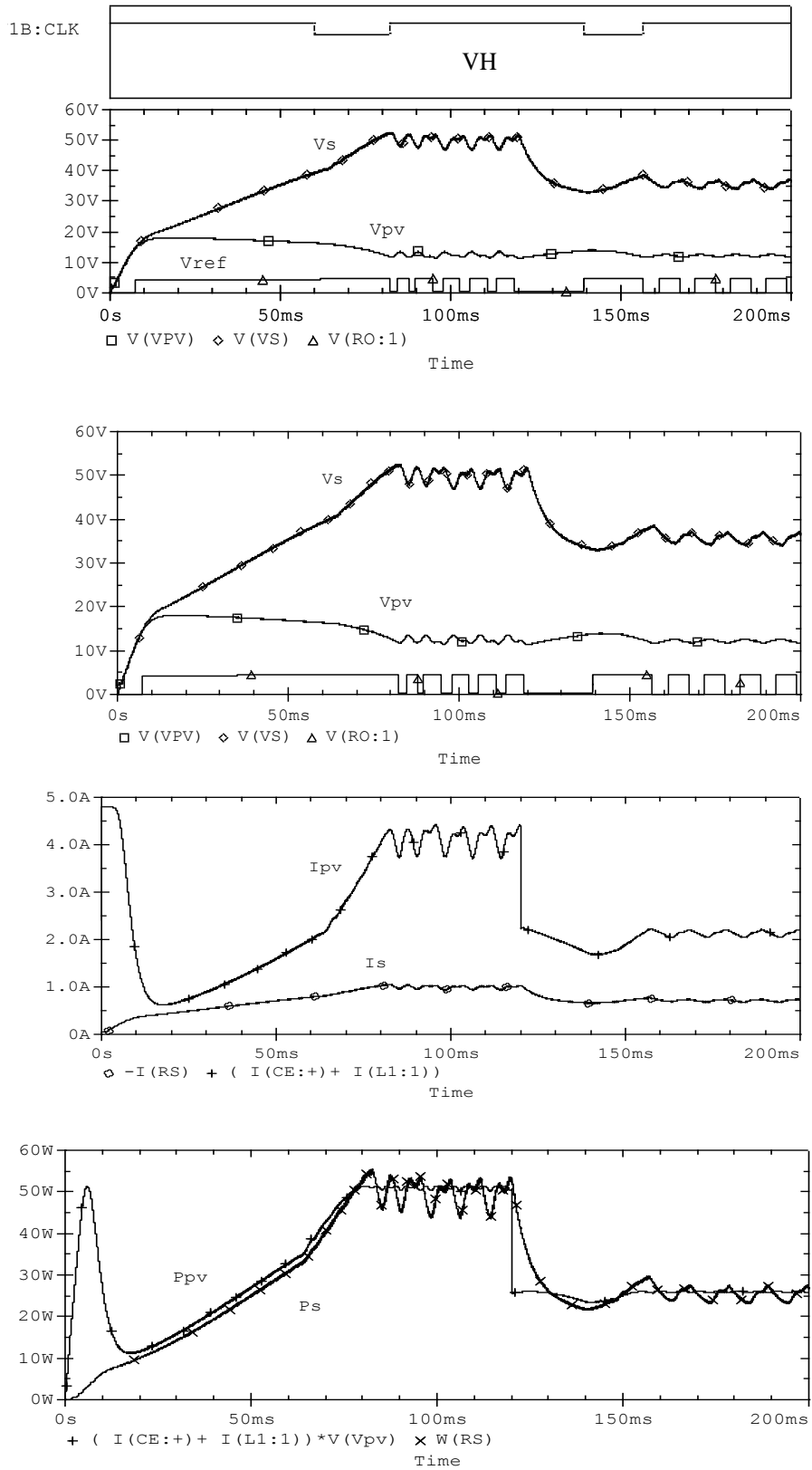


**Figure 13.** Pspice simulations of the clock signal (VH) of the Flip-Flop of the CDSCS circuit, electrical quantities (voltage, current, power) at the input and Output of the boost converter following the variation of the solar radiation from 1000 to 500 W/m<sup>2</sup>, Rs, 50 Ω.

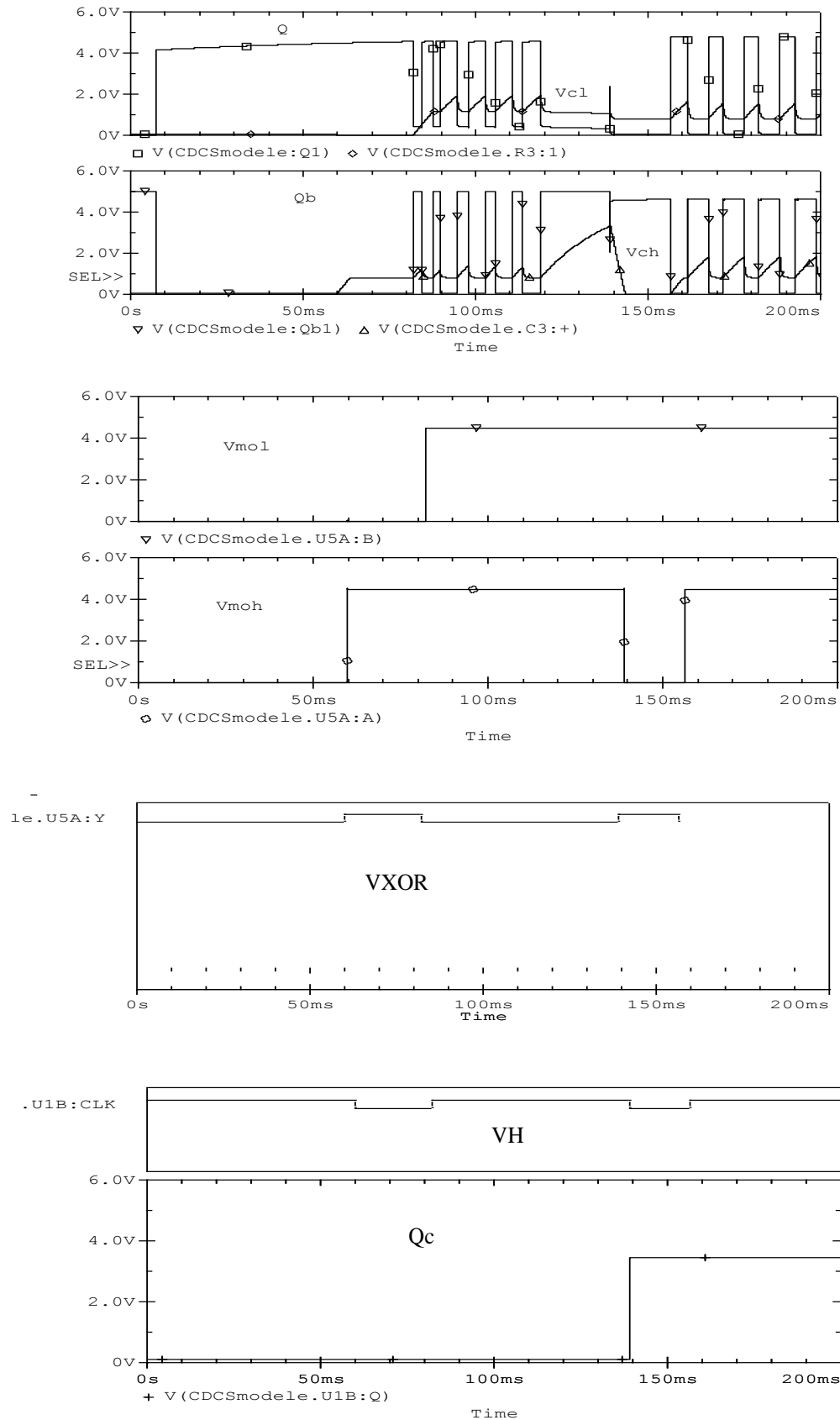


**Figure 14.** Typical simulations in Pspice of operation of the CDCS circuit blocks (Figure 7) when the change in solar radiation from 1000 to 500 W/m<sup>2</sup>. Rs, 50 Ω.



**Figure 15.** Photovoltaic panels SP75 (300 Wpeaks) installed at the laboratory.

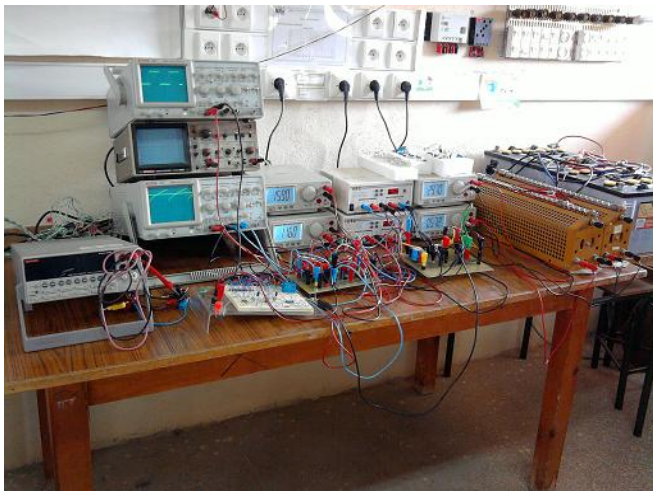


**Figure 16.** Measuring equipments set up to characterize the PV panels and photovoltaic systems.

then the system oscillates around the new optimal electrical quantities that correspond to the solar radiation of  $500 \text{ W/m}^2$ . The output of the upper monostable switches to the unstable state (Up) and the clock signal to the up state until the next divergence.

## EXPERIMENTAL RESULTS

### Experimental procedures

PV Panels SP75 of peak powers 300 Wp and measuring equipments completely automated (2700 Keittley Multimeter/Data acquisition system connected to the PC) which was the subject of our study is represented in Figures 15 and 16. The Multimeter Kheithley can take measurements on 20 channel differentials multiplexer during all the day. Various measurements are treated and analyzed according to the Pspice simulator. DC-DC

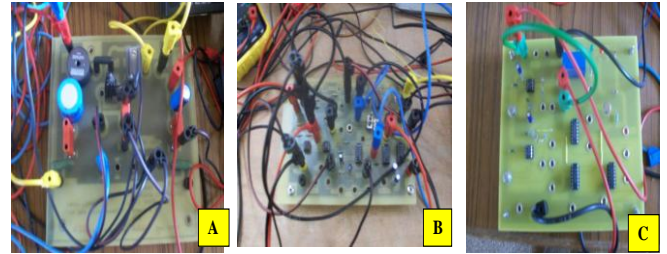


**Figure 17.** Photographs of the charts realized at the laboratory. A, DC-DC converter of the Boost type; B, analogical MPPT command; C, CDCS circuit.

converter (Boost), MPPT command and CDCS circuit dimensioned, designed and realized in this work are represented in Figure 17.

### Optimization of the regulation of photovoltaic (PV) system by maximum power point tracking (MPPT) command

In order to validate the results of simulations and the good performance of PV system realized at the laboratory (Figure 17), we experimented the electric operation of the PV system during sunny and cloudy days when the load is formed by two batteries (12 V, 115 Ah each one) in series or a resistive variable load. We analyzed the operation and the optimization of PV system provided with MPPT command, without CDCS circuit, by varying time constant of the fast ( $\tau_R$ ) and slow ( $\tau_L$ ) integrators on one hand and on the other hand, the time constant ( $\tau_a$ ) of the RoCo integrator (Figure 6).

### Influence of the time constants on the operation of photovoltaic (PV) system

Figures 18 and 19 illustrate the typical experimental results and of simulation of the optimum of PV panel concerning the influence of the fast time constants ( $\tau_R$ ), slow ( $\tau_L$ ) and  $\tau_0$  on the electric quantities of PV system in the case of two batteries in series. In the case of a resistive load, similar results are obtained, with oscillations of large amplitude slightly at load. The results of Figures 18 and 19 shows:

1) When the time constants  $\tau_R$  and  $\tau_L$  are remote and the time constant of the integrator (Ro, Co) is small, then the amplitude of the oscillations are more pronounced. Under these conditions, the system becomes fast and imprecise. The experimental electrical quantities do not oscillate around those of the optimal PV generator: an important swerve is obtained between the experiment and the optimum, in particular the extract of duty cycle

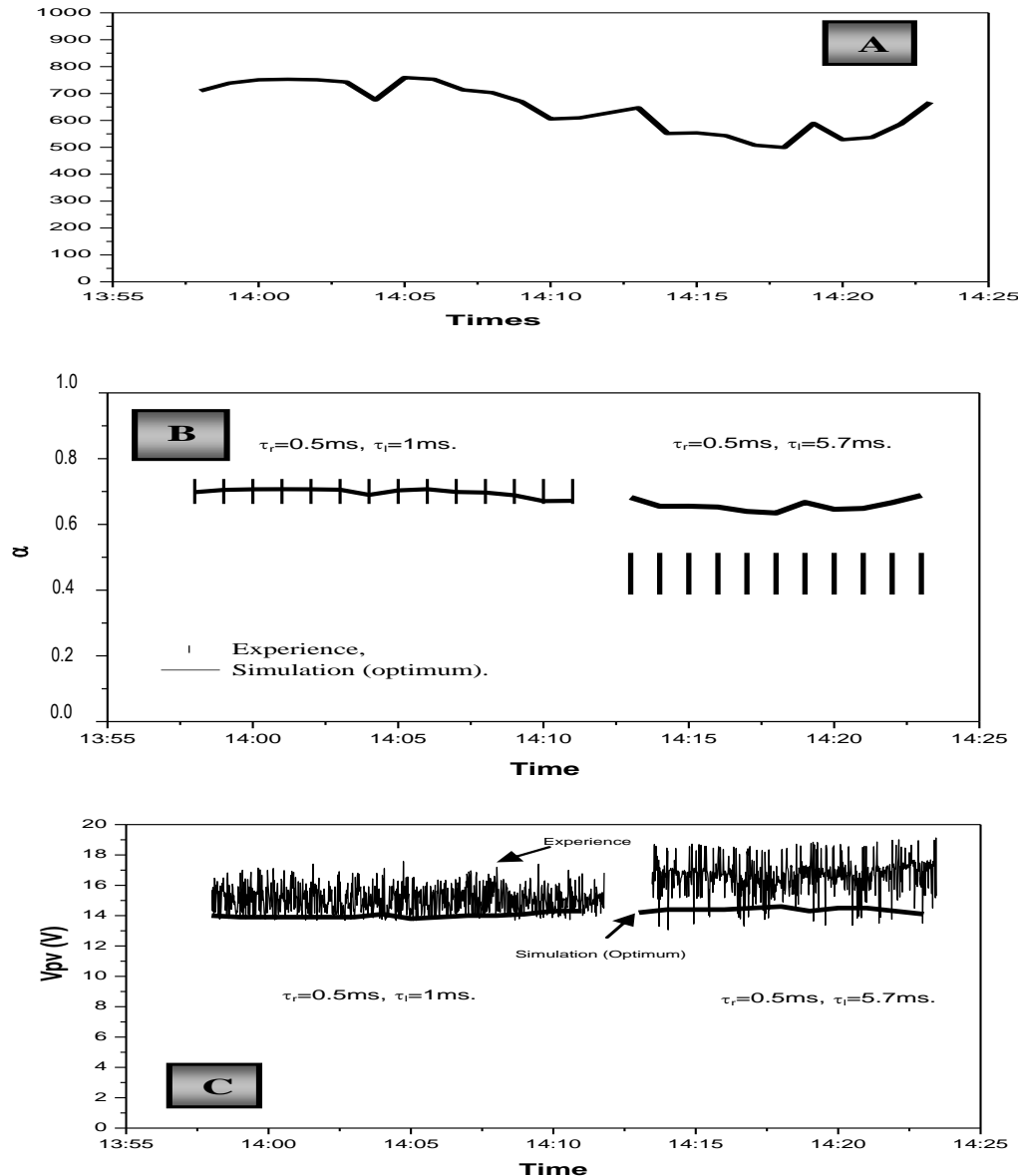


**Figure 18.** Influence of time constants  $\tau_r$  and  $\tau_l$  on the electric quantities of PV panel in the case of two batteries in series (24 V). On the Figures B to E are shown the simulation results (Optimum) in Pspice. T, 24°C; A, Solar radiation; B, duty cycle; C, voltage ( $V_{pv}$ ).

( $\alpha$ ) of PWM signal.

2) When the time constants of slow integrators ( $\tau_L$ ) and fast ( $\tau_R$ ) are close and the time constant of the integrator ( $R_o, C_o$ ) is important, the oscillation amplitude decreases. Under these conditions the system becomes precise. The experimental electrical quantities oscillate around those of the optimal PV generator. The extract of duty cycle ( $\alpha$ ), experimental and simulated PWM signal show such precision.

All results show that the designed PV system performs when the time constants of the first comparator (1) are close and the time constant of the second comparator (2)

is important enough (Figure 6). Therefore, these integrators play an important role in the functioning, dynamics and stability of the system around its MPP.

#### Optimized operation of the PV system on both Q and Qb output of Flip-Flop of the MPPT command

We analyzed the operation of the PV, taking into account previous results, when RoCo integrator is connected either to the Q output or Qb output of the Flip-Flop of the MPPT command (Figure 6). The results are shown in

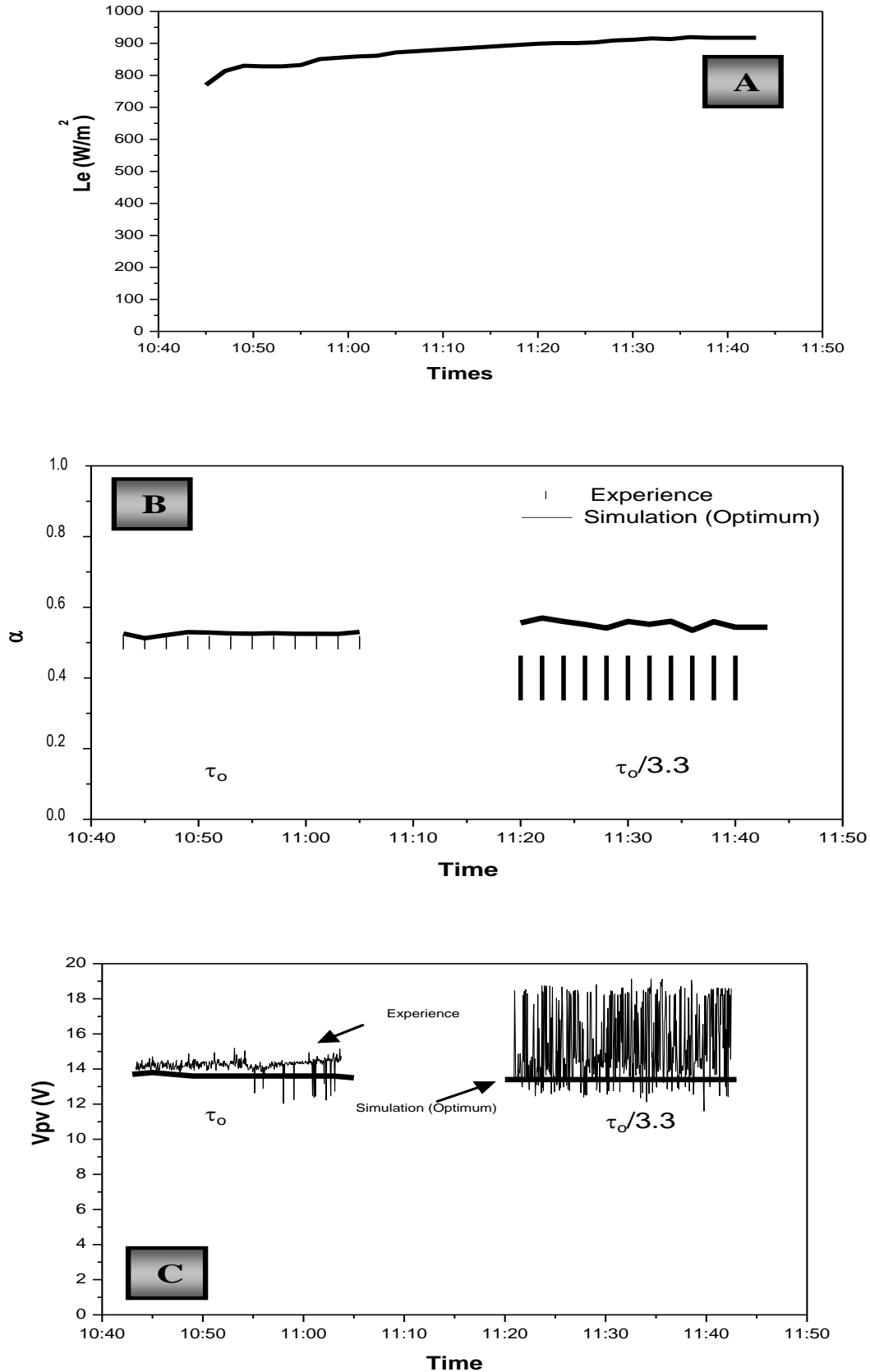


**Figure 19.** Influence of time constant ( $\tau_0$ ) of RoCo integrator on the electric quantities of PV panel in the case of two batteries in series (24 V). T, 24°C; A, Solar radiation; B, duty cycle; C, voltage (V<sub>pv</sub>).

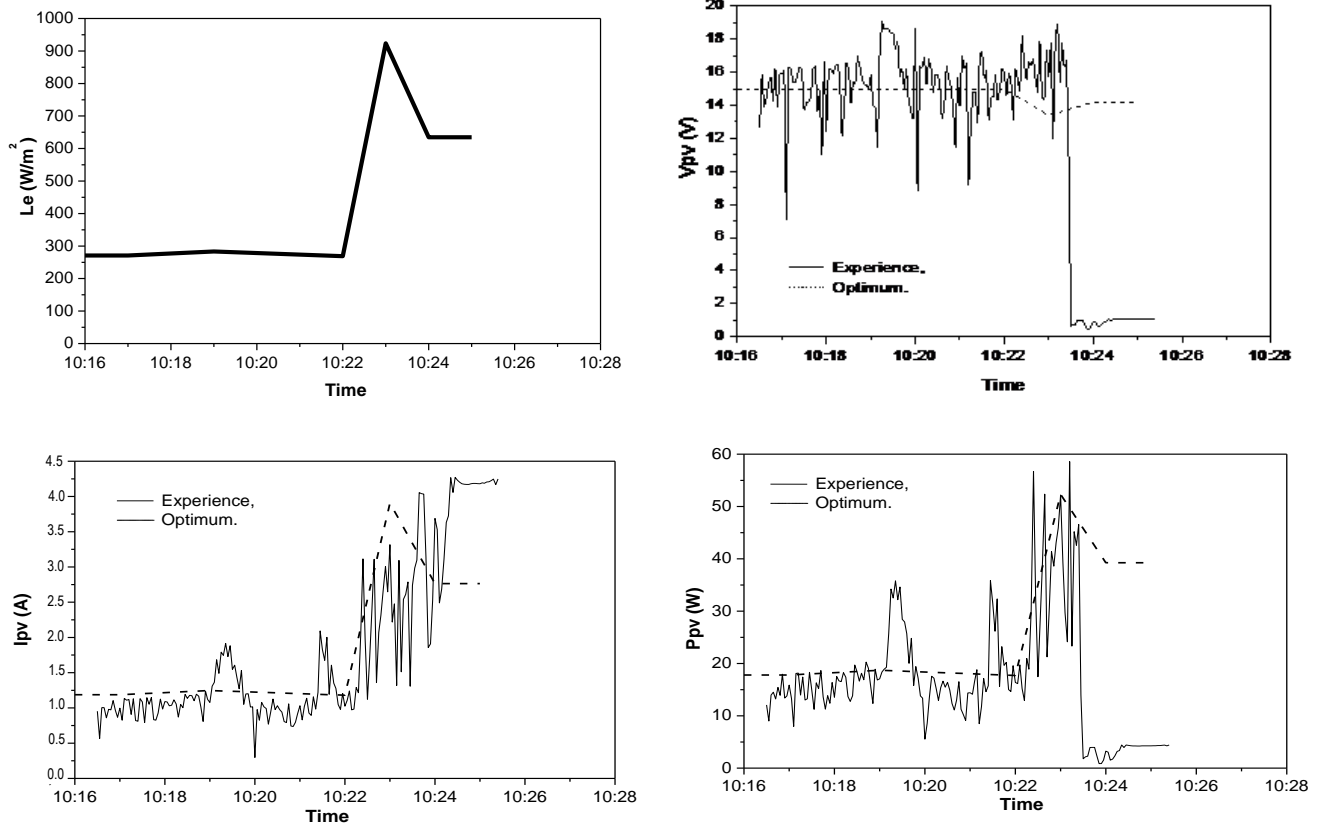


**Figure 20.** Solar irradiation, experimental and simulated (optimum) of the duty cycle and electrical quantities of the PV panel (voltage and power) during a typical operation of the PV system to the outputs Q and Qb of Flip-Flop MPPT command. T, 24°C; Rs, 50 Ω.

Figure 20. On the same figures, we have represented the optimal electrical quantities simulated from the Pspice simulator. It appears in one hand that the operation of the system is practiced the same on both Q outputs and Qb, and in the other hand, on the optimal operation of PV panel. Therefore, both Q outputs and Qb of Flip-Flop can be used to improve the operation of PV system by the CDCS detection circuit of dysfunction (Figure 7).

#### **Divergence of the photovoltaic (PV) system in consequence of the abrupt variations of solar irradiation and load**

We characterized the process of divergence of the PV system on a cloudy day and having variable solar irradiation. We have followed the evolution of the electrical quantities of the PV panel and those of the load during the phase variation of solar irradiation. Typical results obtained when the solar irradiation varies from 300 to 900 W/m<sup>2</sup>, then at 650 W/m<sup>2</sup> are shown in Figure 21. On the same Figure 21B to D, we represented the optimal electrical quantities simulated in Pspice. It appears that:

- 1) There is good agreement between experiment and simulation.
- 2) When the solar irradiation is stable around 300 W/m<sup>2</sup>, the electrical quantities of the panel oscillate around the MPP of the PV panel:  $V_{pv} = 15$  V,  $I_{pv} = 1.3$  A,  $P_{pv} = 19$  W.
- 3) During the abrupt increase in solar radiation, the electric quantities of the PV panel increase and reach the new MPP point corresponding to solar irradiation 900 W/m<sup>2</sup>:  $V_{pv} = 14$  V,  $I_{pv} = 4.2$  A,  $P_{pv} = 58$  W.
- 4) When decreasing the solar radiation at 650 W/m<sup>2</sup>, PV panel loses its MPP and diverges towards the conditions from the closed circuit ( $V_{pv} \cong 0$  V,  $I_{pv} \cong 4.4$  A,  $P_{pv} \cong 0$  W). During this phase, as shown in Figure 21C, PV system diverges and the power provided by PV generator is practically null.

All results show that perturbation of the PV system by the abrupt increase and then decrease in solar irradiation causes the divergence of the optimum operation of the PV panel. The operation of the PV system during the perturbation sequence is shown in Figure 22. The divergence of the system is obtained when the solar radiation varies from 900 to 650 W/m<sup>2</sup>. During this last phase, the fast power ( $P_r$ ) varies without so that it has

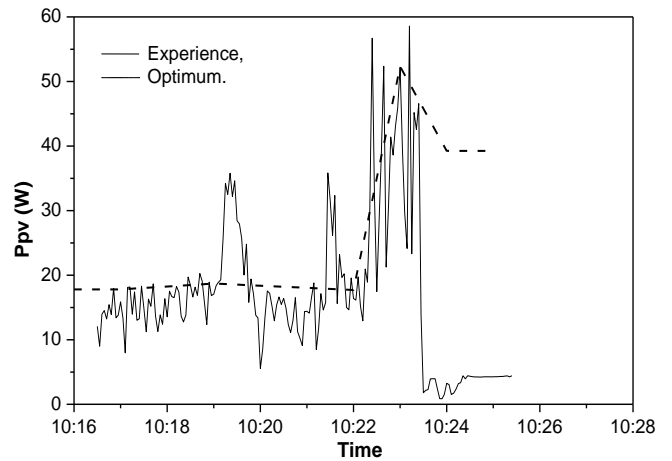
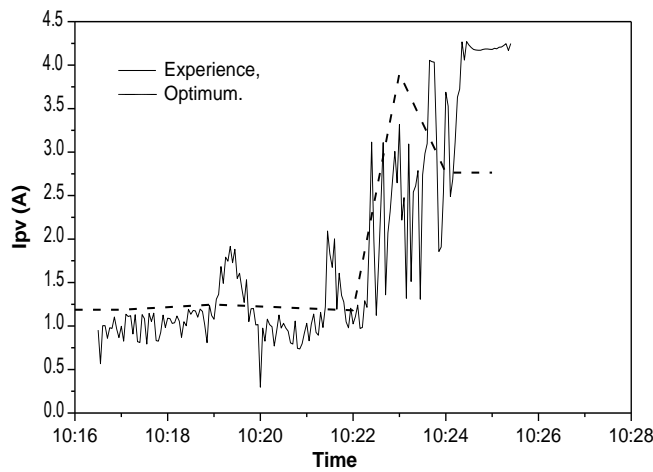
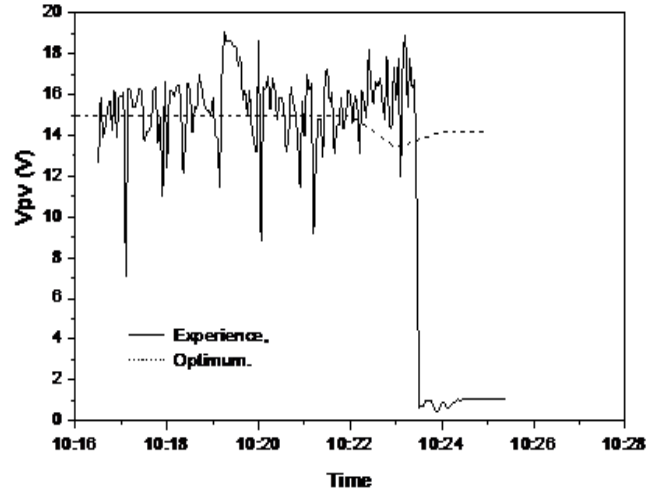
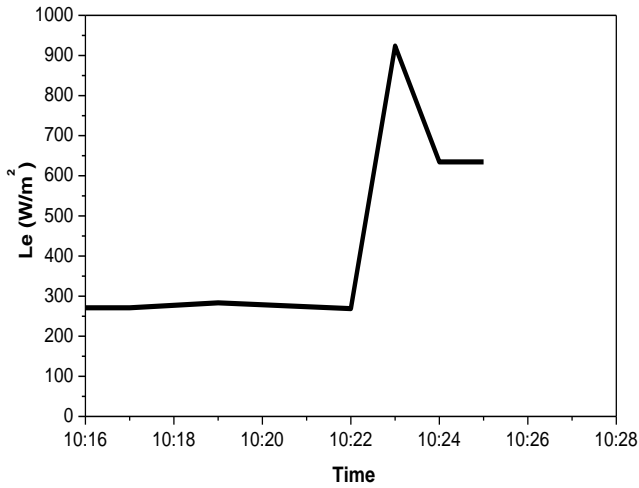


**Figure 21.** Solar irradiation, experimental and simulated (optimum) of the electrical quantities (voltage and current power) of the PV panel in an abrupt change of solar radiation. T, 24°C; Rs, 50 Ω.

crossing with the delayed power (PI) (Figure 6). As a result, the system diverges toward closed circuit conditions.

**Divergences and convergences of the photovoltaic (PV) system**

In the theoretical part, we showed the divergence of the PV system when RoCo integrator is connected to an output (Q or Qb) of the Flip-Flop of the MPPT command, then the reconnection of this integrator on the other output (Qb or Q). This later changes the direction of the displacement of the operation of PV generator and the convergence to its new MPP.

In the following paragraph, we analyze the divergence and convergence of the PV system when the switching of the connection of the RoCo integrator on the outputs Q or Qb of Flip-Flop of the MPPT command is manually

carried out (without CDCS circuit) or automatic (via CDCS circuit).

**Divergence and manual convergence of the photovoltaic (PV) system (without CDCS circuit)**

We studied the divergence and the manual convergence of PV system due to an abrupt change of the load. This switching is carried out via a relay connected between the output of the Flip-Flop of command MPPT and the RoCo integrator (Figure 6). In Figure 23, we represented a solar irradiation of 750 W/m<sup>2</sup>, experimental results of electrical quantities at input and output of the DC-DC converter and the duty cycle in the case of an abrupt change of load from 50 to 25 Ω and 25 to 50 Ω. On the same Figure 23, we represented the optimal electrical quantities simulated in Pspice and the connection status of the RoCo integrator to the output of the Flip-Flop (Q or

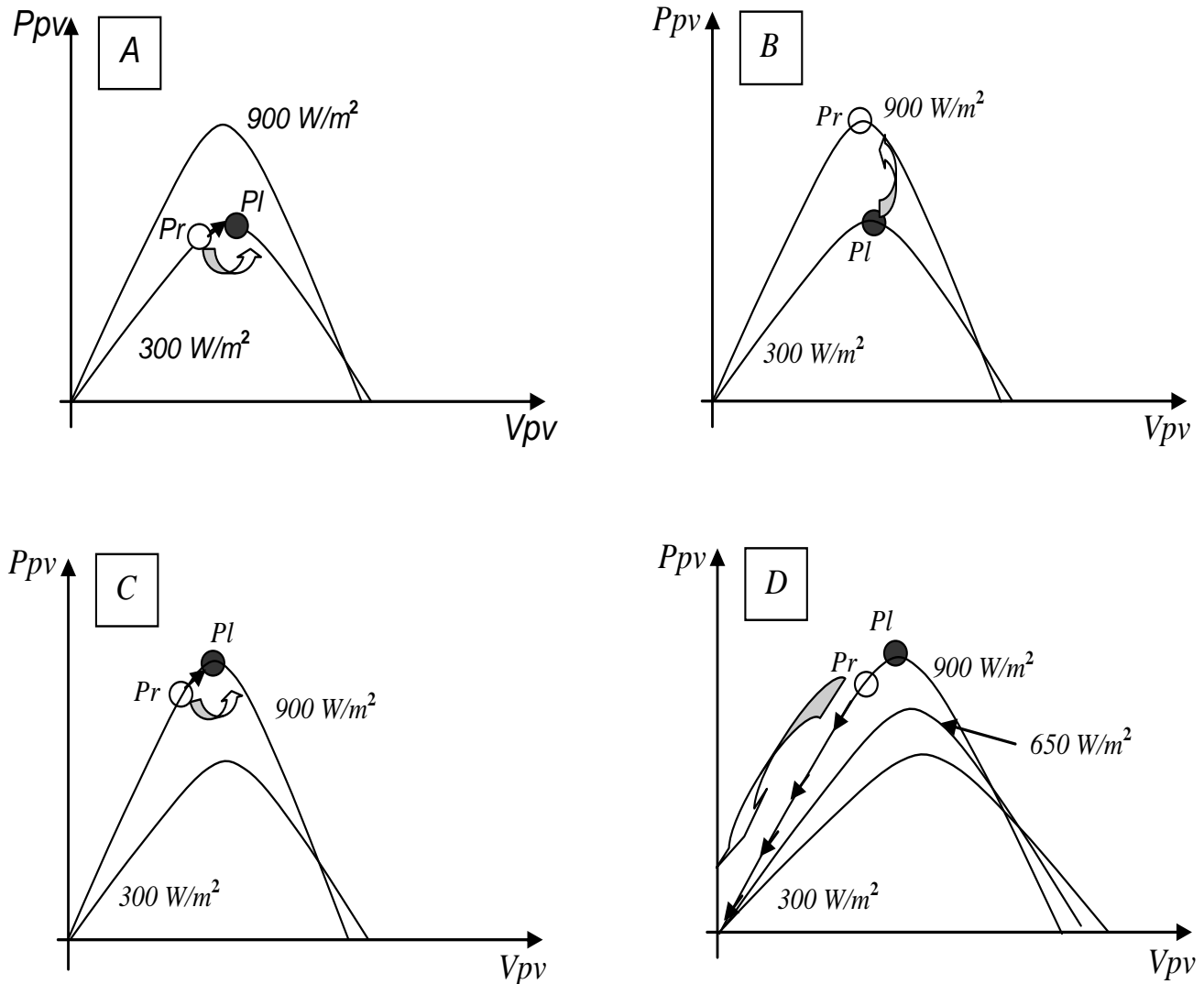


**Figure 22.** Evolution of the MPP (fast and delayed power) PV panel due to changes in the solar irradiation of Figure 21. A, Solar radiation of  $300 \text{ W/m}^2$ ; B, variation from  $300$  to  $900 \text{ W/m}^2$ ; C, solar radiation of  $900 \text{ W/m}^2$ ; D, variation from  $900$  to  $650 \text{ W/m}^2$ .

Qb). Also, on Figure 23C, we represented the form of the output signals Q and Qb of the Flip-Flop. It appears:

- 1) Optimum operation, corresponding to the load  $50$  and  $25 \Omega$ , follow-up of a divergence toward open circuit conditions at each load changes.
- 2) When a divergence, the manual switching from an output to another of the Flip-Flop of MPPT command converge PV system around the MPP.
- 3) When the load changes from  $50$  to  $25 \Omega$ , the PV system diverges when RoCo integrator is connected to the Q output of the Flip-Flop. In this case, the Q output is set to '0'. The switching of the connection of the RoCo integrator on the Qb output of the Flip-Flop, which is in state '1' can as well change the direction of movement of the operating point of PV generator, and therefore convergence to the MPP corresponding to the  $25 \Omega$  load.

4) When the load changes from  $25$  to  $50 \Omega$ , the PV system diverges when RoCo integrator is connected to the Qb output of the Flip-Flop. In this case, the Qb output is set to '0'. The switching of the connection of the RoCo integrator on the Q output of the Flip-Flop, which is in state '1', can as well change the direction of movement of the operating point of PV generator and therefore, the convergence to the MPP corresponding to the load of  $50 \Omega$ . All results obtained shows that PV system provided with an analogical MPPT command loses its MPP during an abrupt load change. Manual switching of the connection of the RoCo integrator of an output (Q or Qb) to another (Qb or Q) allows the change of moving the operating point of PV generator and consequently its convergence to the new MPP. In the following, we analyze this convergence through the automatic CDCS circuit.

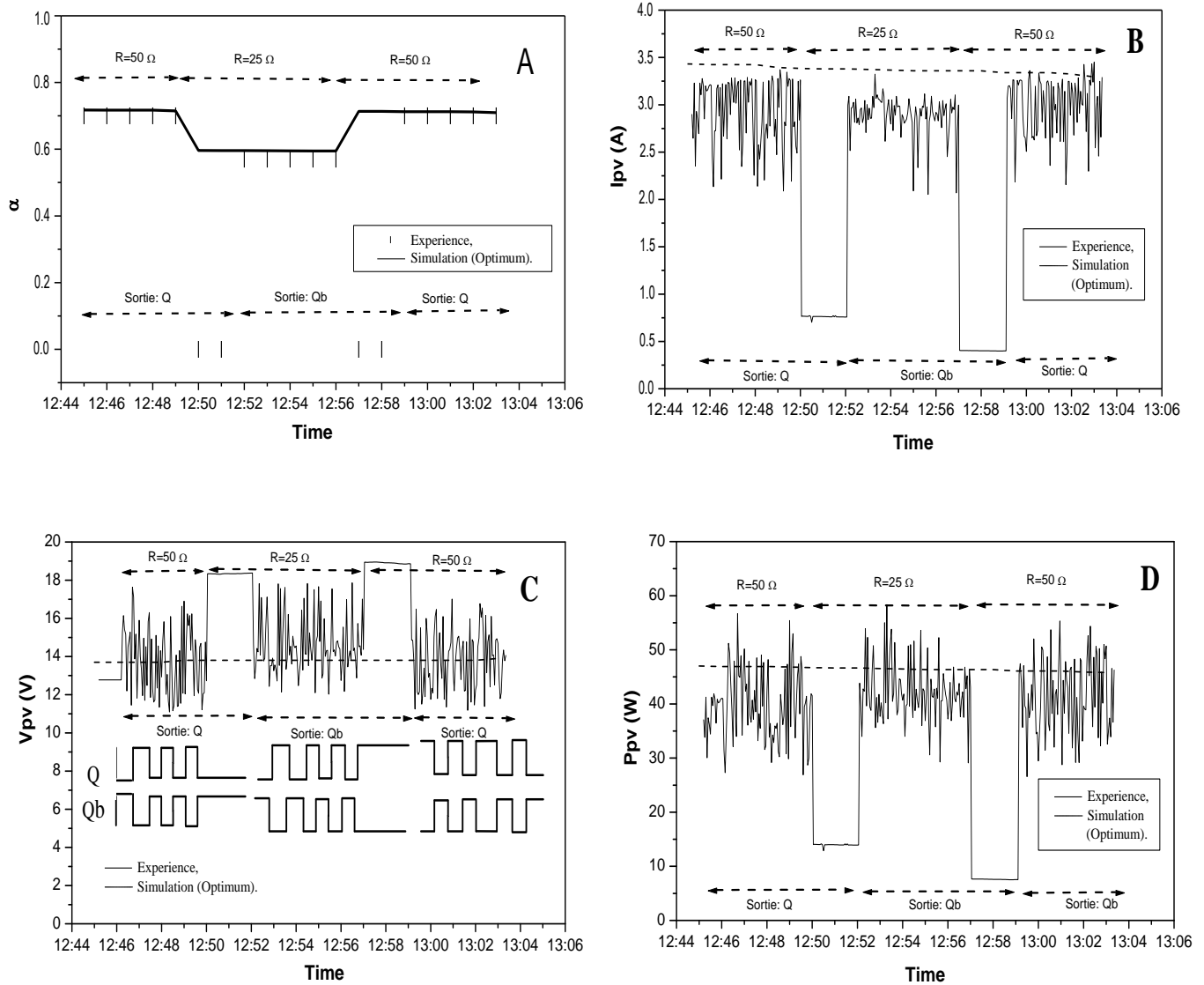


**Figure 23.** A, Duty cycle and electrical quantities; B, voltage; C, current; D, power) of PV panel, experimental and simulated (optimum), during an abrupt variation of the load with the switching on Q or Qb of the Flip-Flop of MPPT command.

**Divergence and automatic convergence of the photovoltaic (PV) system in the presence of the circuit of dysfunction and convergence the system (CDCS) circuit**

**Operation of CDCS circuit:** We experimented the operation of CDCS circuit (Figure 7), noting the various internal signals of the CDCS circuit by the digital oscilloscope in both cases of normal and divergence operation of the PV system. The results are shown in Figures 24 and 25. It appears that:

1) When the normal operation of the PV system is around the point MPP, the output Q (Qb) of the Flip-Flop of the MPPT command switches between the states 'Up' (down)

and 'down' (Up) (Figure 24A and B). As soon as the two monostable receive these signals (Q and Qb), their outputs switch to the unstable state (Up) (Figure 24C and D). Also, under these signals (Q and Qb), since PNP transistors of CDCS circuit blocks and leads, then the C3 and C5 capacitors of two monostable (Figure 7) are slowly loaded and unloaded (Figure 24E and F). The signal at the output of the XOR gate is at down state (Figure 24G) and that of the clock of the flip-flop of the CDCS circuit is in state 'Up' state (Figure 24H). The state 'up' of this clock signal reflects the normal operation of the PV system around the MPP. This result is in very good agreement with that obtained in Pspice simulator.  
 2) When the system diverges (due to changes in solar irradiation or load), the Q and Qb outputs of the Flip-Flop

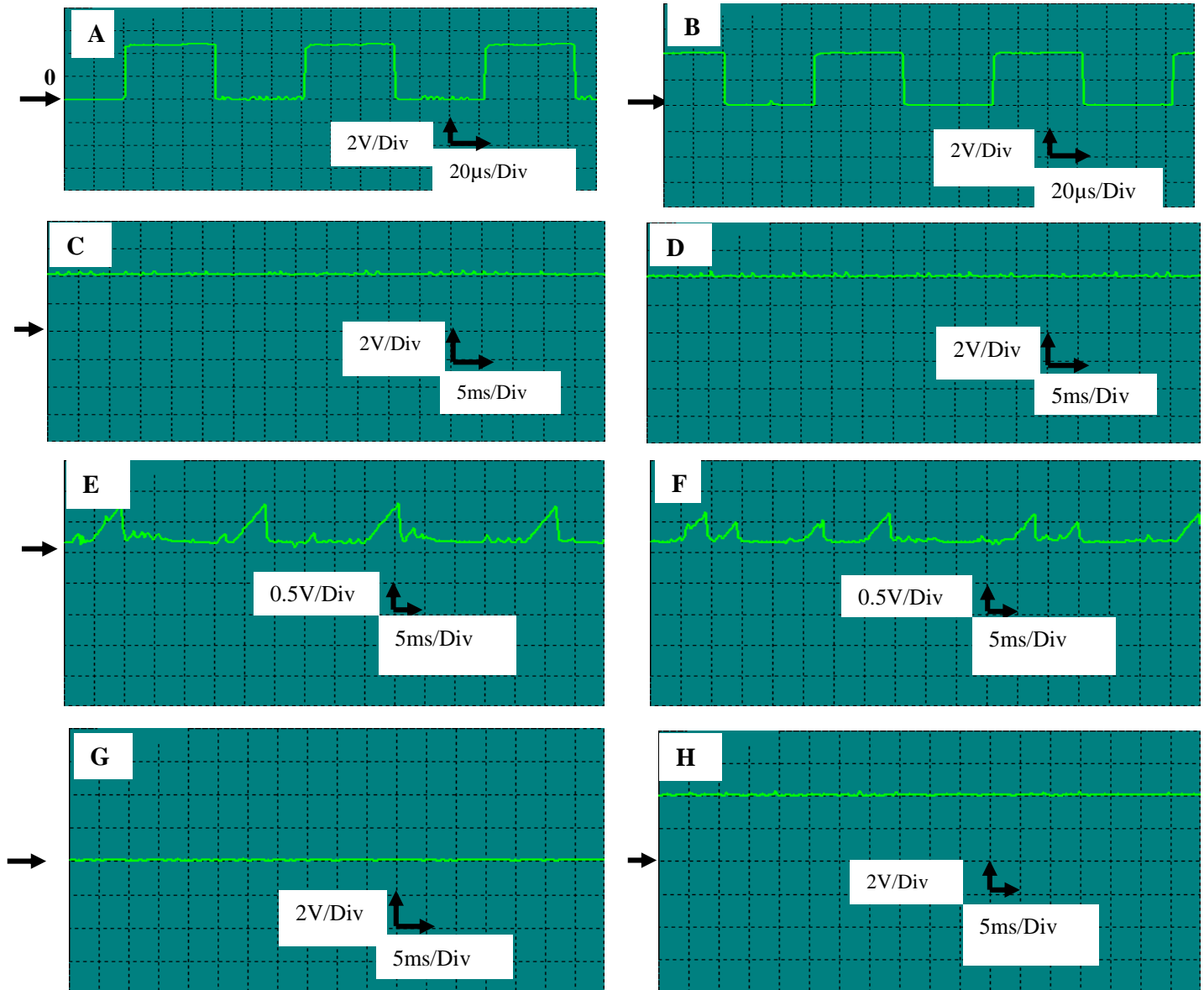


**Figure 24.** Typical form of the signals of the CDCS circuit. A and B, Q and Qb output of the Flip-Flop of the MPPT command; C and D, outputs of the two monostable; E and F, C1 and C3 capacitors; G, output of the XOR unit; H, clock of the Flip-Flop of the CDCS circuit.

of the MPPT command block. The capacitor of the transistor which receives the 'up' state continues to charge until it reaches  $2/3V_{cc}$  (Figure 25A). In our case, we fixed a time of load of about 30 ms (Equation 1). Consequently, the clock signal of the Flip-Flop switches to the state '0' (Figure 25B), demonstrating the detection of the dysfunction of the system, and the output of this Flip-Flop changes state. This change of state switches the connection of the RoCo integrator of MPPT command of an output to the other of the Flip-Flop of MPPT command. The operating point of PV generator changes direction of displacement in order to converge to the new MPP. When the system oscillates around the MPP, the

output Q (Qb) of the Flip-Flop of the MPPT command switches between the states 'Up' (down) and 'Up' (Up) (Figure 24A and B), and the clock signal CDCS circuit switches to state '1' (Figure 25B).

The results obtained here show the good performance of CDCS circuit during a normal functioning of PV system, the divergence and convergence of the system following an eventual change of the load and the solar irradiation. For each case of operation, the results are in good agreement with those obtained in the Pspice simulator. Therefore, the CDCS circuit designed and carried out during this work can be used in a PV installation provided with an analogical MPPT command

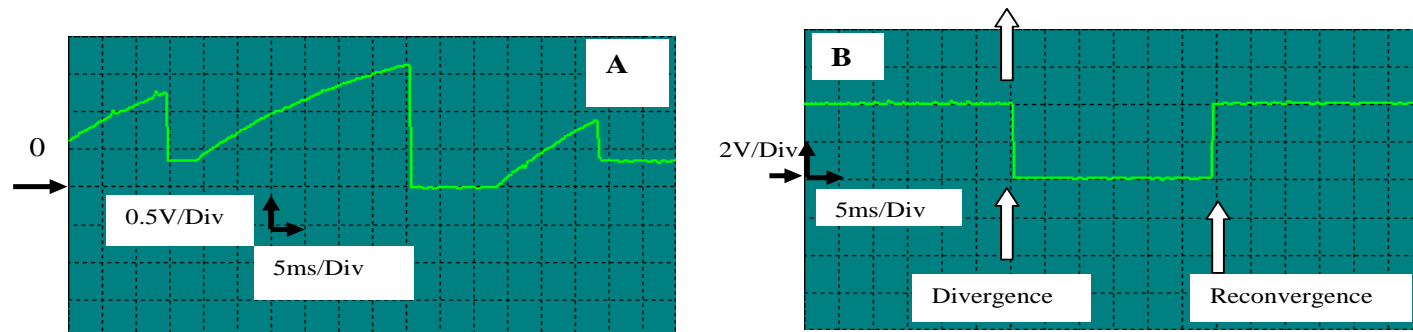


**Figure 25.** Typical forms of signals at capacitor terminals C1 or C3 (A) and clock of the Flip-Flop of CDCS circuit (B) when a detection of divergence and convergence to a MPP.

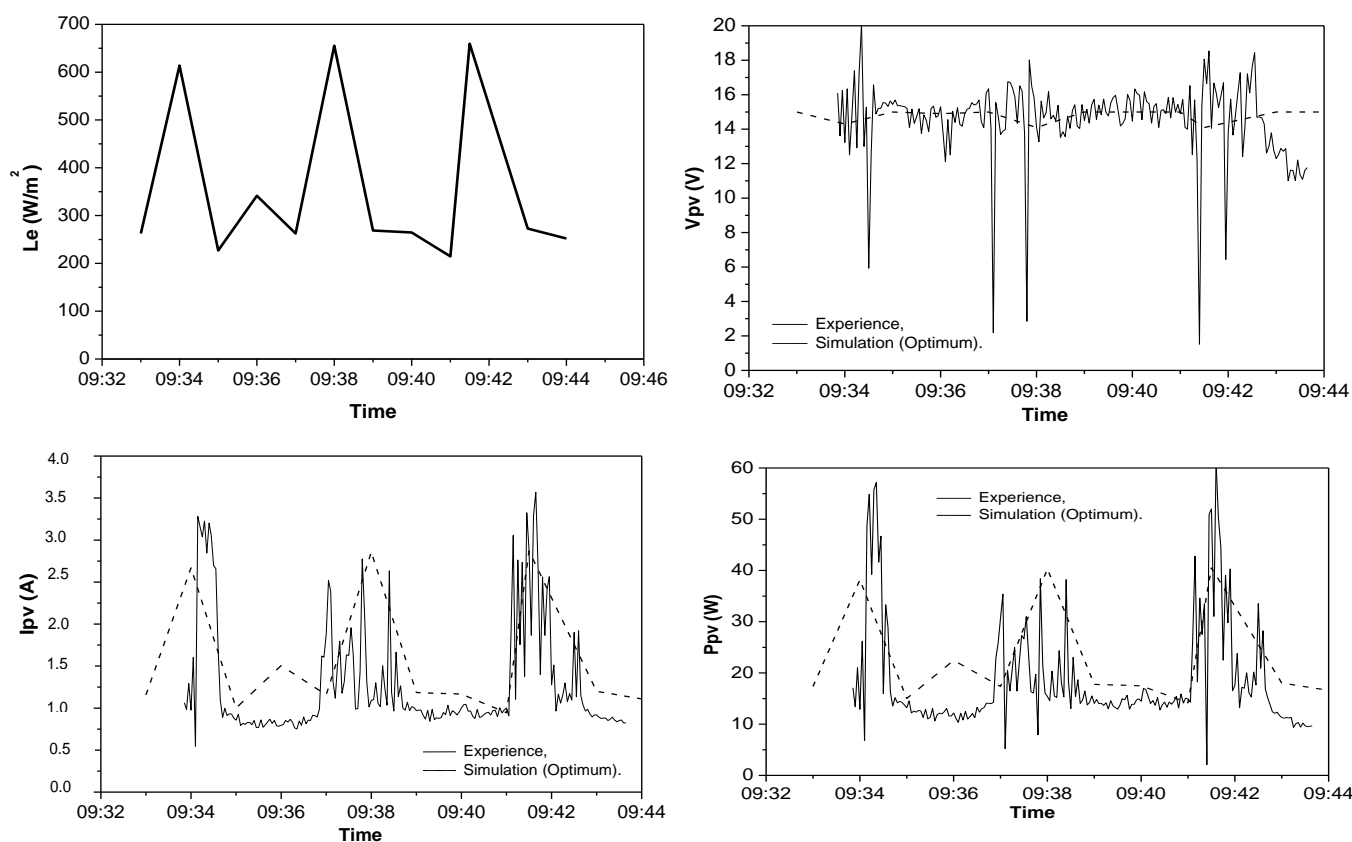


**Figure 26.** Solar irradiation and electrical quantities (voltage, current and power) of the PV when the PV system provided with the MPPT command and CDCS circuit undergoes an abrupt variation of the solar irradiation. T, 24°C.

in order to detect an eventual dysfunction while ensuring optimal operation. Using this circuit, the PV system operates under optimum conditions independently of load and weather conditions changes.

**Operation of photovoltaic (PV) system in the presence of the circuit CDCS:** We have experimented the complete PV system provided with the MPPT command and CDCS circuit on a cloudy day. Specifically,

we analyzed the functioning of the system, when there are abrupt changes of solar irradiation and load. The experimental results and simulated (optimum) in Pspice are presented in Figures 26 and 27. In the case of load changes, we presented on the plots of the Figure 27 the values of the load (50 or 25 Ω), it appears:

- 1) A good agreement between experiment and simulation.

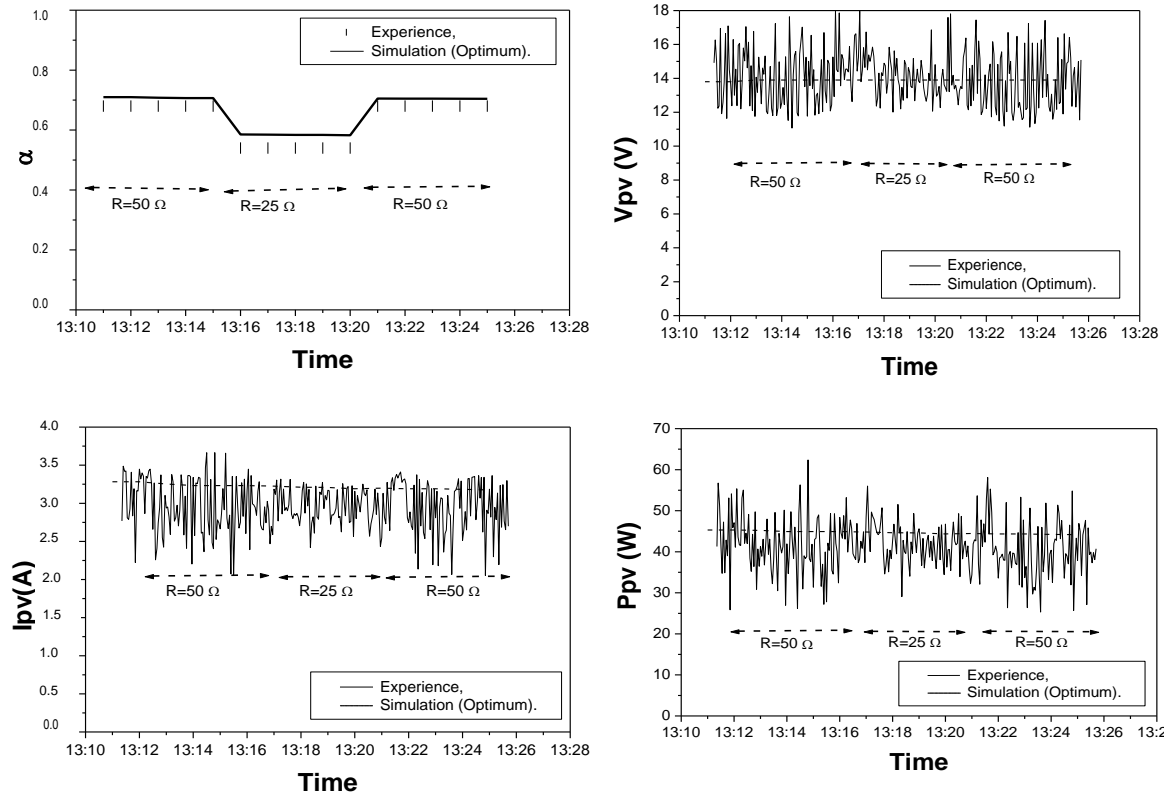


**Figure 27.** Duty cycle and electrical quantities of the panel (voltage, current and power) experimental and simulated in Pspice (optimum) for a PV system provided with an MPPT command and a CDCS circuit disturbed by variations abrupt of the load (R). Le,  $750 \text{ W/m}^2$ , T,  $24^\circ\text{C}$ .

2) The electrical quantities of the panel and load oscillate around those optimal.

3) Every variation of the solar radiation or the load, the CDCS circuit detects the dysfunction and ensures optimum operation. These results were checked throughout the day.

The results obtained here show the good performance of CDCS circuit and PV system. Every perturbation of the PV system by varying the solar radiation or the load, the PV system does not lose its MPP. The circuit detects the dysfunction and switches connection of RoCo integrator of an output to another of the Flip-Flop of the MPPT command. Consequently, the PV panel works all day at optimum power. Next, we evaluate from the simulator Pspice, the power losses after one day of operation of complete PV system.

### Operation of complete photovoltaic (PV) system during one entire day

In order to validate the operation and the performances of the complete PV (generator, Boost DC-DC converter, MPPT command, CDCS circuit and load (resistive or batteries) in Figure 6, we followed the operation of the

system thus, carried out during a sunny day, with some cloudy periods and an ambient temperature of  $22^\circ\text{C}$  in the morning and  $28^\circ\text{C}$  in the afternoon. In Figure 28, we represented the experimental and simulated in Pspice (optimum) results: variation of solar radiation, duty cycle ( $\alpha$ ) of the signal that controls the power switch, voltage at the input and output of the converter ( $V_{pv}$  and  $V_s$ ), current at the input and output of the converter ( $I_{pv}$  and  $I_s$ ), power delivered by PV panel ( $P_{pv}$ ) and power at the load ( $P_s$ ). All these results show that:

1) The solar radiation varies during the day from  $245$  to  $794 \text{ W/m}^2$ . The maximum solar irradiation is obtained at the midday and is of the order of  $794 \text{ W/m}^2$ .

2) The experimental electric quantities at the input and the output of Boost DC-DC converter are in very good agreement with the optimum characteristics of PV panel simulated in Pspice.

3) During the day, the maximum power at the input and the output of the Boost converter are reached about the middle of the day.

4) During the operation of the system's detection of the divergence, the PV system detects the dysfunction and the convergence to the new MPP.

In order to ensure the good performance of PV system

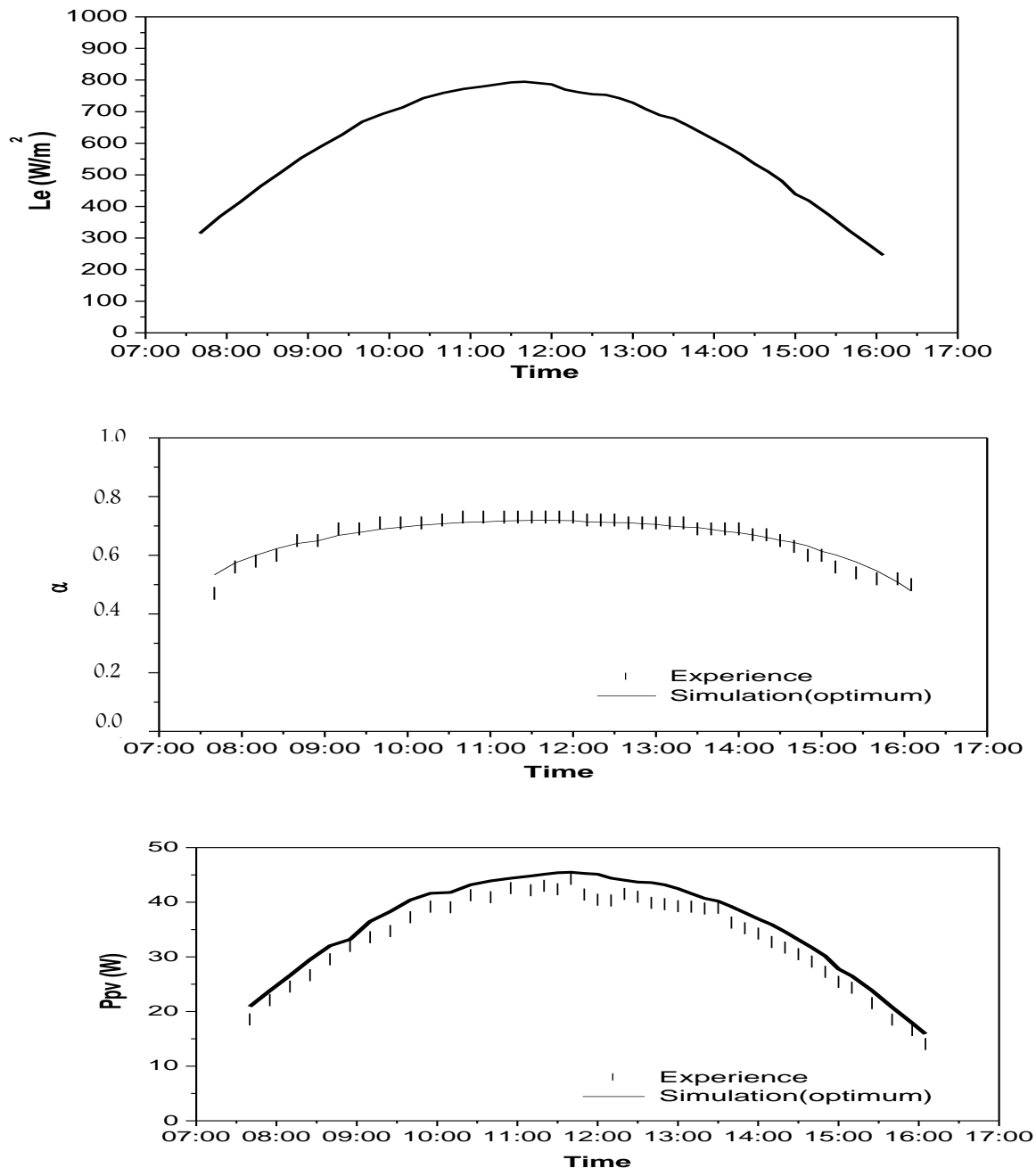


**Figure 28.** Solar radiation, experimental and simulation (Optimum) of the duty cycle and the electric power at the input and the output of DC-DC converter of PV system provided with command MPPT and CDCS circuit. T, 24°C.

during the day, we have represented in Figure 29 the experimental efficiency and the instantaneous power losses of the PV system. The efficiency of the converter satisfactory varies during the day between 85 and 90%. The power losses of the PV system do not exceed 10%. The average production of energy during the day is about 281.30 Wh. From the simulation results of the optimal operation of PV generator, the energy losses of the PV panel are estimated less than 7%.

Finally, all results obtained here show very well the validation of the simulation results in Pspice as well as the good performance of experimental PV system of our PV system of Figure 6. During all the day, the PV panel operates under optimum conditions with each divergence CDCS circuit it detects and convergence the global system to the MPP. These results and the low energy losses show the good performance of the PV system designed and carried out in this work.

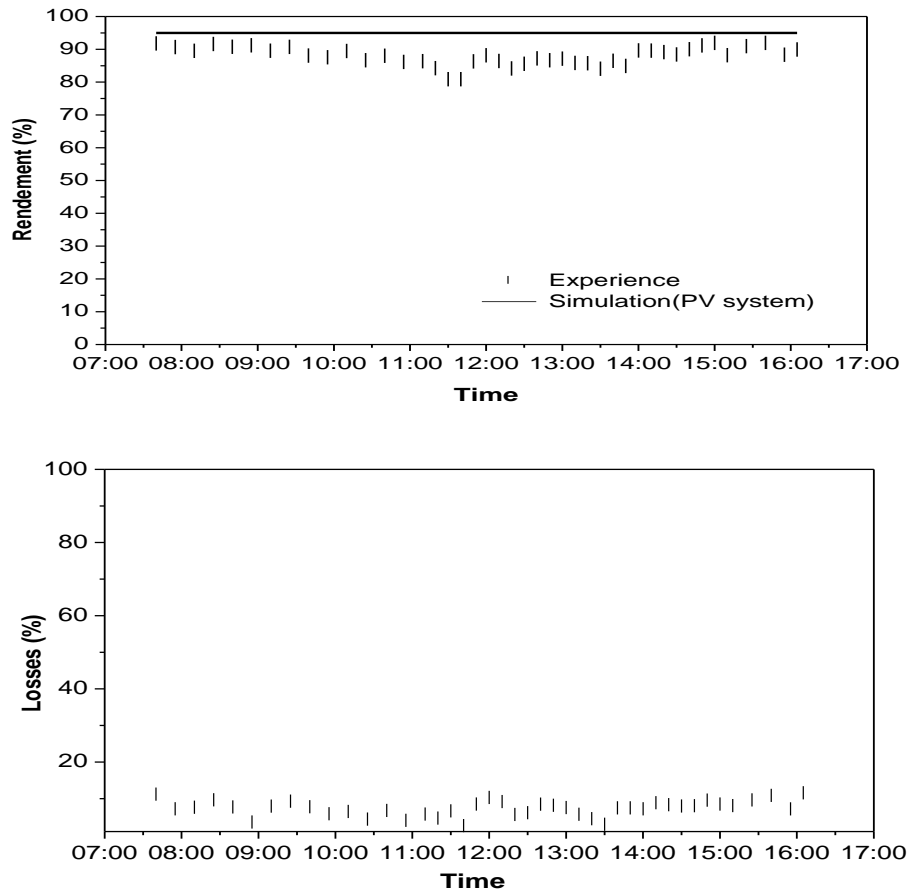


**Figure 29.** Experimental and simulated (Optimum) efficiency, experimental power loss of the PV system provided with the MPPT command and CDCS circuit. T, 24°C.

## CONCLUSION

In this paper, we analyzed in the Pspice simulator, and experiments operation of a PV system consists by a PV generator, a Boost DC-DC converter and an analogical MPPT command provided with a CDCS while ensuring an optimal operation. We have analyzed on one hand the optimum operation of the system provided with MPPT command, and on the other hand the complete system provided with MPPT command and CDCS circuit during an abrupt variation of the load and the solar radiation. The results obtained show that:

- 1) The optimum operation of the system depends on the parameters of MPPT command. By taking adequate parameters, the system oscillates around the MPP in perfect agreement with the results of simulations in Pspice.
- 2) The CDCS circuit plays properly its role during an abrupt variation of the load or solar irradiation. This circuit detects, after a time fixed by the user, the dysfunction of the system and converge it instantaneously to its new MPP without restarts of the PV system.

In order to validate all results obtained, we have experimented the system realized during a sunny day. We have checked very well the optimum operation of PV system all the day without divergence and energy losses. With each divergence of the system, following perturbations (solar radiation...), CDCS circuit detects dysfunction and converge it to the MPP. From the Pspice simulator, the produced energy losses are estimated lower than 7%. These results and the good performance of DC-DC converter (efficiency of 90%) show the optimization and the reliability of PV system designed and carried out in this work. Consequently, the PV system designed, carried out and optimized in this work can be used in a PV installation in order to reduce energy losses due to the installations and perturbation (solar radiation, loads...).

This work was pursued particularly to evaluate the prototypes carried out on PV installations of high power (higher than 1KW). In achieving our short and long terms, we did the following:

- 1) The study improved the structure of the MPPT command by providing the CDCS circuit in the case of DC-DC buck.

2) Valorization on two stations (pumping and lighting). These stations are installed in the framework of United Nations program (PUND), Morocco Art Gold (2008 2 ENV O O) in the Douar Zragta of the municipality of the prefecture Issly Oujda Angad.

## ACKNOWLEDGEMENTS

This work is supported by du Programme Thématique d'Appui à la Recherche Scientifique (PROTARS III) 'D43/06, Cooperation Maroc-Belge « Commission Universitaire Institutionnelle», CUI-Oujda 2008-2012 (Activité Eau et Environnement / sous-activité Energies Renouvelables) and Projet PGR : Energies Photovoltaïques.

**Nomenclature:** **PV**, Photovoltaic, **MPP**, maximum power point; **V<sub>pv</sub>**, output photovoltaic panel (V); **I<sub>pv</sub>**, photovoltaic panel current (A); **I<sub>cc</sub>**, short-circuit current (A); **I<sub>s</sub>**, saturation current (A); **R<sub>s</sub>**, series photovoltaic cell resistance ( $\Omega$ ); **I<sub>opt</sub>**, optimum photovoltaic panel current (A); **V<sub>opt</sub>**, optimum photovoltaic panel voltage (V); **V<sub>oc</sub>**, open circuit voltage (V); **L<sub>e</sub>**, solar radiation ( $W/m^2$ ); **MPPT**, maximum power point tracking; **PWM**, pulse width modulation; **CDCS**, circuit of the dysfunction and convergence the system.

## REFERENCES

- Azmi Aktacir M (2011). Experimental study of a multi-purpose PV-refrigerator system. *Int. J. Phys. Sci. ISI Indexed J.*, ISSN 1992-1950, 6(4): 746-757.
- Damak A, Guesmi A, Mami A (2009). Modeling and fuzzy control of a photovoltaic-assisted watering system, *J. Eng. Technol. Res.*, 1(1): 007-013
- Dasgupta N, Pandey A, Ashok K, Mukerjee (2008). Voltage-sensing-based photovoltaic MPPT with improved tracking and drift avoidance capabilities, *Solar Energy Mat. Solar Cells.* (92): 1552-1558.
- Dorin P, Toma P, Stefan D, Cristina M, Brian M (2011). A novel maximum power point tracker based on analog and digital control loops. *Solar Energy*, 85: 588-600.
- El Ouariachi M, Mrabti T, Kassmi Ka, Yaden F, Kassmi K (2010). Analysis, Optimization and Modelling of Electrical Energies Produced by the Photovoltaic Panels and Systems, 18th Mediterranean conference on control and automation, IEEE ISBN: 978-1-4244-8091-3, pp. 1614-1619.
- El Ouariachi M, Mrabti T, Tidhaf B, Kassmi Ka, Bagui B, Kassmi K (2009b). Regulation of the electric power provided by the panels of the photovoltaic systems, *Int. Confere. Multimedia Computing Syst., ICMCS'09*, IEEE ISBN: 978-1-4244-3757-3, pp. 454-459.
- El Ouariachi M, Mrabti T, Tidhaf B, Kassmi Ka, Kassmi K (2009a). Regulation of the electric power provided by the panels of the photovoltaic systems, *Int. J. Phys. Sci., ISI Indexed J.*, ISSN 1992-1950, 4(5): 294-309.
- Ellouze M, Gamoudi R, Mami A (2010). Sliding mode control applied to a photovoltaic waterpumping system, *Int. J. Phys. Sci., ISI Indexed J.*, ISSN 1992-1950, 5(4): 334-344.
- Enrique JM, Andujar JM, Bohorquez MA (2010). A reliable fast and low cost maximum power point tracker for photovoltaic applications. *Solar Energy*, 84: 79-89.
- Gules R, Pacheco JDP, Hey HL (2008). A Maximum Power Point Tracking System With Parallel Connection for PV Stand-Alone Applications, *IEEE Trans. Indust. Elect.*, (55): 7.
- Houssamo I, Locment F, Sechilariu M (2010). Maximum power tracking for photovoltaic power system: Development and experimental comparison of two algorithms, *Renewable Energy* (35): 2381-2387. <http://datasheet.abcelectronique.com/456/456-21050-0-NE555>.
- Huang BJ, Sun FS, Ho RW (2006). Near-maximum-power-point-operation (nMPPO) design of photovoltaic power generation system, *Solar Energy* (80): 1003-1020.
- Kalirasu A, Dash SS (2011). Modeling and Simulation of Closed Loop Controlled Buck Converter for Solar Installation. *Int. J. Comput. Elect. Eng.*, 2(3): 1793-8163.
- Kassmi K, Hamdaoui M, Olivie F (2007a). Characterization of photovoltaic panels, design and optimization of a photovoltaic system for better use of solar energy, *Renewable Energy*, United Nations Educational, Scientific and Cultural Organization, UNESCO Office in Rabat, Office multi countries in the Maghreb, renewable energy in Morocco, the debate starts. Morocco. ISBN9954-8068-2-2, pp. 87-110.
- Kassmi K, Hamdaoui M, Olivie F (2007b). Design, optimization and realization of photovoltaic systems for better use of Solar Energy, *Energy Management in the Construction and Renovation of Buildings*, Industrial Centre of Advanced Studies, "CESI", Rouen, France.
- Kuei-Hsiang C, Ching-Ju Li (2010). An intelligent maximum power point tracking method based on extension theory for PV systems, *Expert Syst. Appl.*, 37: 1050-1055.
- Mrabti T, El Ouariachi M, Kassmi K, Kassmi Ka, Bagui F (2009). Regulation of the electric power of the photovoltaic generators with DC-DC converter (Buck type) and MPPT command, *International Conference on Multimedia Computing and Systems, ICMCS'09*, IEEE ISBN: 978-1-4244-3757-3, pp. 322-326.
- Mrabti T, El Ouariachi M, Kassmi K, Tidhaf B (2010c). Characterization and modelling of the optimal performances of the marketed photovoltaic panels, *Moroccan J. Condenser Mater. MJCM*, ISSN: 1114-2073, 12(1): 7-12.
- Mrabti T, El Ouariachi M, Kassmi Ka, Kassmi K, Tidhaf B (2010b). Characterization and Fine Modeling of Electric Operation of Photovoltaic Panels, *Arch. Phys. Res.*, 1(1): 1-11.
- Mrabti T, El Ouariachi M, Yaden F, Kassmi Ka, Kassmi K (2010a). Characterization and Modeling of the Electrical Performance of the Photovoltaic Panels and Systems, *Journal of Electrical Engineering: Theory Appl.*, 2(1-2010): 100-110.
- Narendran E, Harikrishnan G, Ashokkumar KCR, Malathi R (2010). Simulation analysis on high step-up DC-DC converter for fuel cell system, *J. Eng. Technol. Res.*, 2(9): 168-176.
- Neil D'Souza S, Luiz Lopes AC, XueJun Liu (2010). Comparative study of variable size perturbation and observation maximum power point trackers for PV systems, *Elect. Power Syst. Res.*, 80: 296-305.
- Salameh ZM, Dagher F, Lynch WA (1991). Step-Down Maximum Power Point Tracker for Photovoltaic Systems. *Solar Energy*, 4(46): 279-282.
- Shmilovitz D (2005). On the control of photovoltaic maximum power point tracker via output parameters, *IEE Proc.-Elect. Power Appl.*, 2(152): 239-248.
- Shraif MF (2002). Optimization and measurement chain Photovoltaic Energy Conversion into Electrical Energy, PhD from the University Paul Sabatier of Toulouse, France.
- Uyigue E, Archibong EO (2010). Scaling-up renewable energy technologies in Africa, *Int. J. Phys. Sci., ISI Indexed J.*, ISSN 1992-1950, 2 (8) :130-138.
- Yaden MF, El Ouariachi M, Mrabti T, Kassmi Ka, Tidhaf B, Chadli E, Kassmi K (2011). Design and realization of a photovoltaic system equipped with a digital MPPT control. *J. Renewable Energies, CDER*, ISSN: 1112-2242, 1 (14): 171-186.